arXiv:hep-ph/0111043v1 5 Nov 2001

Edinburgh 2001/19
LAPTH-873/01
November 2001

A NEXT-TO-LEADING ORDER STUDY OF PION-PAIR PRODUCTION & COMPARISON WITH E706 DATA

T. Binoth[b], J. Ph. Guillet[a], E. Pilon[a] and M. Werlen[a]

[a] *Laboratoire d'Annecy-Le-Vieux de Physique Théorique LAPTH, Chemin de Bellevue, B.P. 110, F-74941 Annecy-le-Vieux, France*

[b] *Department of Physics and Astronomy, University of Edinburgh, Edinburgh EH9 3JZ, Scotland*

Abstract

We discuss the production of pion pairs with a large invariant mass in hadronic collisions. We present a study based on a perturbative QCD calculation at full next-to-leading order accuracy, implemented in the computer programme *DIPHOX*. We provide a comparison of various predictions with the corresponding observables measured by the E706 fixed target experiment. Discrepancies between data and next-to-leading order calculation are carefully analysed. We classify the theoretical next-to-leading order distributions with respect to their infra-red sensitivity, and explain which distributions need improvements. Further, we comment on the energy scale dependences of non pertubative effects.

1 Introduction

Quantum Chromodynamics (QCD) is now accepted as the theory of the strong interaction. With the starting run II of the Fermilab Tevatron, and the forthcoming Large Hadron Collider (LHC) at CERN, QCD is entering a new area associating improved precision measurements with more accurate calculations. This concerns not only a refined study of the strong interaction itself and, in particular, the ability of perturbative QCD to describe high energy phenomena precisely, but also the accurate prediction of sensitivities in Higgs boson and expected new physics searches. Both need an accurate understanding of respective signals and backgrounds, which are heavily affected by QCD radiative corrections. Meanwhile, the proper understanding of the large amount of data collected by fixed target experiments remains rather challenging. In all these respects, the production of neutral pion pairs with a large invariant mass is an interesting phenomenon. This process has been recently measured by the fixed target E706 Experiment [1] at the Fermilab Tevatron. The study of this process and the examinations of the various observables which have been measured are instructive for several reasons.

First of all, it is interesting to compare the ability of perturbative QCD to describe single pion and pion pair production respectively. In particular, one can identify the observables for which non perturbative effects are negligible and the QCD improved parton model based on collinear factorisation can be safely used, and examine otherwise when it fails and why. In this respect, loosely speaking, inclusive enough correlation observables with symmetric selection cuts are less sensitive to non perturbative effects such as, e.g. a k_T kick, than one particle inclusive distributions [2], especially at fixed target energies. Dipion observables thus provide a good opportunity to cross-check the consistency of the sets of parton-to-pion fragmentation functions $D_{i\to\pi^0}(z, M_f^2)$, such as those given in Ref. [3] and the more recent ones in Ref. [4], which are available in the literature[1]. Both these sets have been extracted from data on hadronic final states in e^+e^- annihilation. They are given by analytical ansätze whose parameters were fitted in the range $0.1 \leq z \leq 0.9$ but which are tightly constrained[2] only in $0.1 \leq z \leq 0.7$. In particular, the gluon-to-pion fragmentation functions are not much constrained because the subprocesses involving gluons in e^+e^- annihilation appear at higher order in the perturbative expansion. Instead, subprocesses involving outgoing gluons contribute already at lowest order in hadronic collisions. Therefore the contributions from gluon fragmentation in hadronic collisions are not negligible and large uncertainties on their magnitude may affect quantitative predictions.

In addition, the production of π^0 pairs, together with the production of pairs $\gamma\pi^0$, where γ is itself a prompt photon, is the dominant background against which the experiments measuring prompt photon pairs have to fight. The expression "prompt photon" means that such a photon does not come from the decays of a hadron such as π^0, η, etc. produced at large transverse momentum. This background is especially worrisome in collider experiments, such as the Collider Detector at Fermilab (CDF) [6] and D0 [7] experiments at the Fermilab Tevatron, where the pions cannot be all reconstructed event by event. In addition, these two processes of $\gamma\pi^0$ and $\pi^0\pi^0$ production represent an important fraction of the so-called reducible background to the search of neutral Higgs bosons in the channel $H \to \gamma\gamma$ in the intermediate mass range 80 – 140 GeV at the CERN Large Hadron Collider (LHC) [8–11]. Since the jet-jet cross section is about eight orders of magnitude larger than the expected Higgs boson signal for a standard model Higgs boson, this reducible background is overwhelming before any selection cut is imposed. Stringent isolation cuts are applied in order to reduce this background severely and make prompt photons measurable. Nevertheless, it is a theoretical challenge to understand the remaining background at a quantitative level. In this respect,

[1] Similar consistency checks for the set determined in [4], especially for the gluon fragmentation functions, have been presented in Ref. [5] in the case of hadro- and photo-production of single inclusive charged hadrons.

[2] To be precise, regarding pions, the authors of [4] determine fragmentation functions into charged pions then deduce the ones into neutral pions relying on isospin symmetry.

the understanding of π^0 pair production in the fixed target energy range will allow one to transport this knowledge to collider energies [12] using the factorization property of perturbative QCD.

In the present article, we present a phenomenological study of π^0 pair production at Next-to-Leading Order (NLO) accuracy in perturbative QCD, based on the computer code *DIPHOX* [13]. In section 2 we briefly describe the theoretical content on which the present study is based. We then compare *DIPHOX*-based theoretical results with data of the E706 experiment in section 3. Section 4 is then dedicated to a detailed phenomenological discussion of the various observables measured in π^0 pair production. The aim of this phenomenological study is 1) to test the ability of the theoretical framework used to describe various correlation observables that have been measured by the E706 experiment, 2) to identify and understand the possible discrepancies between theory and data for these observables, and 3) to examine how the sensitivity to non perturbative effects, which limit the predictive power of the perturbative approach, evolves as the 'hardness' of the probes increases. To this purpose we classify the various observables according to their sensitivity to the infrared dynamics. At this occasion, the analysis of the transverse distribution of each pion leads us to reconsider briefly the p_T spectrum in the case of inclusive one pion production as well. Section 5 gathers our conclusions and perspectives. The goal is to foresee how reliable predictions based on our present knowledge can be for dipion production at much higher, collider energies. In a forthcoming paper, we will investigate more specifically our ability to predict the reducible background to the Higgs boson search at LHC in the channel $H \to \gamma\gamma$, relying on the informations obtained in the present study.

2 Theoretical content

The computer program *DIPHOX* on which the present study relies is a Monte Carlo code of partonic event generator type. This code has been designed to describe the production of pairs of particles in hadronic collisions, accounting for all contributing partonic processes at full NLO accuracy. These particles can be prompt photons or hadrons, in particular neutral pions. This code is flexible enough to accommodate various kinematic or calorimetric cuts. Especially, it allows to compute cross sections for isolated $\gamma\pi^0$ and $\pi^0\pi^0$ pairs, for any infrared and collinear safe isolation criterion which can be implemented at the partonic level. The physical content and schematic description of *DIPHOX* has been given in [13], where we have concentrated on the case of diphoton production[3] [14,15]. However, the production mechanisms of fragmentation type involved in diphoton production are exactly the same as the ones at work in the hadroproduction of $\gamma\,\pi^0$ and $\pi^0\pi^0$. Let us remind this point briefly.

A prompt photon may be produced according to two possible mechanisms: either it takes part directly to the hard subprocess (let us call it call "direct"), or it results from the collinear fragmentation of a parton which is itself produced with a large transverse momentum (let us call it "from fragmentation"). Consequently, pairs of prompt photons with a large invariant mass may be produced according to three possible mechanisms: both of them take part directly to the hard subprocess (direct mechanism), or one of them takes part directly to the hard subprocess while the other one results from the fragmentation of a large transverse momentum parton (one-fragmentation mechanism), or else each of them results from fragmentation (two-fragmentation mechanism). For a general discussion of the production mechanisms of prompt photon pairs, see [13]. Similarly, $\gamma\,\pi^0$ pairs with a large invariant mass may be produced according to two possible mechanisms: either the prompt photon takes part directly to the hard subprocess (direct mechanism), or it results from the collinear fragmentation of a parton which is itself produced with a large transverse momentum (fragmentation mechanism).

[3] The acronym *DIPHOX* stands for "diphoton cross sections".

In agreement with the factorisation property - even in the case of reasonable isolation requirements, see Ref. [16] - the partonic subprocesses involved by the one-fragmentation mechanism in prompt photon pair production are the same as the ones involved in $\gamma\,\pi^0$ production when the prompt photon is of the 'direct type'. The only change is the fragmentation functions involved: fragmentation into a photon in the first case, into a pion in the last one. Similarly, the partonic subprocesses involved by the so-called two-fragmentation mechanism in prompt photon pair production are the same as both the ones involved in $\gamma\pi^0$ production when the prompt photon come from fragmentation mechanism, and those involved in π^0 pair production. Therefore, by keeping only the relevant mechanisms, and replacing the fragmentation functions appropriately, *DIPHOX* allows also to study the production of $\gamma\,\pi^0$ as well as of π^0 pairs with a large invariant mass and individual transverse momenta, at full NLO accuracy.

3 Comparison with the E706 data

The E706 experiment [1] studied collisions[4] on various fixed targets (H,Be,Cu) of several beams. They used proton beams at different beam energies, 530 GeV ($\sqrt{S} \simeq 31.55$ GeV) and 800 GeV ($\sqrt{S} \simeq 38.76$ GeV), as well as a 515 GeV π^- beam ($\sqrt{S} \simeq 31.10$ GeV). We have decided to focus on comparisons with data from proton initiated reactions, because the sets of available pion's pdf are rather old and not as reliable as the recent ones for protons. We have also focused on data on Hydrogen and Beryllium targets, because the Beryllium nucleus is still rather small hence nuclear effects are hopefully reduced, in contrast to the case of a Copper target where nuclear effects are more important. We have performed a comparison between our NLO QCD results and data on Hydrogen and Beryllium targets, for protons beam energies of 530 GeV and 800 GeV. We have chosen to present only the comparison with the data obtained in proton-Beryllium for which the statistics is larger than for Hydrogen target. We restrict the presentation mainly to a comparison with data from the collision of the 530 GeV proton beam, in order to limit the proliferation of plots in the article. Similar conclusions have been obtained in the other cases studied.

The NLO QCD predictions presented here are provided by the computer code *DIPHOX* presented in the previous section. Both the theoretical results and the data are expressed 'per effective nucleon' in the Beryllium nucleus (Z=4, A=9), this effective nucleon being defined by the combination '4/9 proton + 5/9 neutron'. The theoretical calculations use the CTEQ5M set [19] of parton distribution functions (pdf) for the proton pdf's, and assume that the neutron pdf's are simply deduced from the ones of the proton by isospin symmetry. The KKP set [4] is used for the fragmentation functions into a pion. Our theoretical results are given for a common scale choice for the renormalisation scale μ, initial state factorisation scale M and final state fragmentation scale M_f equal to $\mu = M = M_f = (3/4)\mu^0$ where $\mu^0 = (P_{T1} + P_{T2})/2$ is the average value of the p_T's of the two pions. At fixed target energies, the scale uncertainties remain pretty large in NLO calculations. We made a rapid investigation[5] of the scale dependence of the predictions around the above choice, using also the two other followings sets of scales: $\mu = M = (1/2)\mu^0$, $M_f = \mu^0$; and $\mu = M = M_f = \mu^0$. The choice $\mu = M = M_f = (3/4)\mu^0$ turns out to accommodate to the data better in the case of

[4] The inclusive hadroproduction of pion pairs has also been studied earlier by the CCOR ISR experiment [17] and the NA24 fixed target experiment [18] at CERN. We choose to focus on the data collected by the E706 experiment, which is more recent and gathers higher statistics.

[5] A comprehensive procedure would be, as in one particle inclusive production, to perform a detailed study of these dependences with respect to μ, M, M_f separately. This would help, at least, in quantifying the scale uncertainties more quantitatively. This would also possibly determine a region of local stability with select a set of optimal scales, invoking the Principle of Minimal sensitivity [20, 21]. At fixed target energies, such an optimal scale choice can be found in the case of single pion inclusive case. However, the surrounding region of local stability is a narrow area sitting on a sharp ridge [22], an unsatisfactory situation. Furthermore, this type of study is quite computer time consuming already in the single particle inclusive case. Its cost becomes prohibitive in the case of correlations in dipion production. Therefore we did not perform such a complete study.

the p_T distribution of each pion, as can be seen in Fig. 2, whereas the higher (lower[6]) scale choice undershoots (overshoots) the data, cf. Fig. 1. In addition, we made comparisons with E706 data in pp collisions with an energy beam of 800 GeV ($\sqrt{S} \simeq 38.76$ GeV), using the same scale choice and reaching similar conclusions. This somewhat legitimates the choice of scales adopted. In this section we display the comparisons between the data and our NLO estimates for the various observables measured by the E706 experiment. A corresponding phenomenological analysis will be presented in the next section. We see that these observables split qualitatively into two groups, according to the degree of agreement or disagreement with the experimental spectra.

3.1 Well described observables

For the given scale choice, the agreement is reasonably good in shape, as well as in magnitude, for the distribution of transverse momentum of each pion in pairs[7] $d\sigma/dp_T$ (Fig. 2), for the invariant mass distribution of pairs $d\sigma/dm_{\pi\pi}$ (Fig. 3) - except in the very first bins at low invariant mass -, for the rapidity distribution of the pairs $d\sigma/dy_{\pi\pi}$ (Fig. 4), and for the distribution in $\cos\theta^*$ (Fig. 5). The variable $\cos\theta^*$ is defined by[8] $\cos\theta^* = \tanh y^*$ where $y^* = (y_1 - y_2)/2$ is half the difference of the rapidities of the two pions in a pair.

The reasonable agreement observed was expected for these observables over the whole measured spectrum. Let us however focus in particular on the distribution $d\sigma/dp_T$. The remarkable fact is that the agreement is fairly good over the totality of the measured spectrum. This may be contrasted with the situation in the case of one-particle inclusive production, measured also by the same experiment, and which was confronted to a NLO calculation in Ref. [22]. Let us first briefly remind the results which were obtained in Ref. [22]. The calculation used the BKK set of parton to pion fragmentation functions [3]. The scales, selected by the application of the Principle of Minimal Sensitivity [20, 21], were close to $p_T/3$. This set of scale somehow maximized the theoretical prediction, and turned out to minimize the discrepancy between the latter and the data. Above $p_T \geq 5.5$ GeV, no large difference between the shapes of the NLO calculation and the data was found. On the other hand, the NLO calculation undershot the data by about 50%. The discrepancy between the NLO result and the data was found larger with other, especially larger scales (a factor 1.8 for the scale choice $p_T/2$). Furthermore, in the lower range of the p_T spectrum below 5.5 GeV, the slope of the data is increasingly sharper than the one of the NLO post-diction as the p_T decreases. On the contrary in the case of the p_T distribution of each pion in pair production, the agreement is reasonably good in shape, and also in magnitude with the intermediate scale choice $\mu = M = M_f = (3/8)(P_{T1} + P_{T2})$ used. One notices that the above scale choice involves higher values (by nearly a factor 2) than the optimal scales in the case of single inclusive production. The agreement in shape is rather robust

[6] One cannot go down to too low scales. Another choice of scale commonly used would be $\mu = M = M_f = (p_{T1} + p_{T2})/4$ (half the average value of the p_T's of the two pions). However the lowest factorisation scale M_0 at which the KKP set starts is $M_0 = \sqrt{2}$ GeV. With the selection cut $p_{T\,min} = 2.5$ GeV on each pion, this choice would lead to a scale that could fall below M_0. Technically, a backward evolution, or, more drastically, the freezing of the pdf's below M_0 can be enforced. However the use of such questionable remedies would induce extra sources of theoretical uncertainties.

[7] According to this definition each event enters twice, i.e.:

$$\frac{d\sigma}{dp_T} = \frac{d\sigma}{dp_{T1}} + \frac{d\sigma}{dp_{T2}}$$

[8] This variable has been initially introduced in the literature in the case of $2 \to 2$ processes, where θ^* is the angle, defined in the center of mass system of the pair, between the direction of the beam and the direction of the pions, emitted back-to-back in this frame. This definition is convenient at lowest order (LO). It is however difficult to extend it in a simple and unambiguous way to processes with more than two particles in the final state, as it is the case in calculation beyond LO in particular. In the case of a $2 \to 2$ process, $\cos\theta^*$ turns out to be equal to $\tanh y^*$. In addition to provide an alternative definition which is manifestly invariant under longitudinal boosts, this identity allows to extend the definition of $\cos\theta^*$ to processes with more than two particles in the final state. This is the definition used by the E706 experiment [1], and the one which we adopt here.

with respect to variations in the arbitrary scales μ, M and M_f, at least within the three common values which we scanned, cf. Fig. 1. Furthermore, the agreement in the case of pair production holds even down to fairly low values of p_T close to $p_{T\,min} = 2.5$ GeV above which the events were experimentally selected, in sharp contrast with the situation in the single inclusive case. This fact may appear somewhat surprising, and even counterintuitive because one may think that the agreement should be better, the more inclusive the observable. This puzzle will be examined in some details in the next section.

3.2 Poorly described observables

In contrary, the NLO approximation is completely inadequate to account for the distribution of azimuthal angle difference between the two pions, $d\sigma/d\phi_{\pi\pi}$ (Fig. 6), and for the distribution $d\sigma/dp_{T\,out}$ (Fig. 7). The variable $p_{T\,out}$ is defined as follows. The direction of the beam axis and the transverse momentum of one of the pions define a plane; the component of the p_T of the other pion which is orthogonal to this plane defines the $p_{T\,out}$ of this pion[9]. The disagreement is also sharp for the transverse momentum distribution of pairs $d\sigma/dq_T$ (Fig. 8). The transverse momentum balance distribution $d\sigma/dZ$ (Fig. 9) is not adequately described by the NLO approximation either, particularly in the region $Z < 1$. The p_T balance variable Z is defined for the pion j by[10] $Z = -(\vec{p}_{T1}\cdot\vec{p}_{T2})/|p_{Tj}|^2$. The shapes of these observables, especially of $\phi_{\pi\pi}$ and $p_{T\,out}$ distributions are notoriously infrared sensitive respectively when $\phi_{\pi\pi} \to \pi$ and $p_{T\,out} \to 0$. Therefore it is not surprising that the NLO calculations do not describe these regions adequately. The noticeable fact is that even the tails of these distributions are unmatched. The NLO estimates fall much too rapidly compared with the data, the former being more than one order of magnitude below the latter. These features will be examined in detail in the next section. Last, in Fig. 3 we notice also the poor account of the very first bins at low invariant mass in the invariant mass distribution by the NLO calculation.

4 A classification of dipion observables

The observables of inclusive pion pair production can be theoretically classified into two main categories, according to their respective infrared sensitivity. This theoretical classification matches with the phenomenological one above, according to the 'degree of agreement (or disagreement)' between the NLO predictions provided by *DIPHOX* for inclusive neutral pion pair production and the recent high statistics data of the fixed target E706 experiment at Fermilab.

The first category which we will consider gathers the observables which are infrared insensitive. By this we mean that the contribution associated with the multiple soft gluon emission is not logarithmically enhanced order by order in perturbation theory. Typical representatives of this class of observables are: the distribution $d\sigma/dp_T$; and $d\sigma/dm_{\pi\pi}$, at least when the invariant mass $m_{\pi\pi}$ is larger than $2\,p_{T\,min}$ (the reason for this restriction will be examined later). Other examples are: the distribution $d\sigma/d\cos\theta^*$; and the rapidity distribution of the pairs, $d\sigma/dY$.

The opposite class gathers the infrared sensitive distributions. The shapes of these distributions are well known to be strongly influenced by multiple soft gluon emission in the vicinity of some 'critical point'. Depending on the observable considered, this critical point may lie at the elastic boundary of the spectrum; or it can stand inside the physical domain. Order by order in perturbation theory the infrared sensitivity is signed by the appearance of large logarithms of Sudakov type which become infinite at the critical point. Among these distributions, one may distinguish between two types. A first family is made of the distributions for which the perturbative calculation is singular at the

[9] In other words, the $p_{T\,out}$ of pion $j = 1, 2$ is equal to $p_{Tj}\sin\phi_{\pi\pi}$. Notice that each event enters twice in this distribution.

[10] In this observable as well each event enters twice.

critical point order by order in perturbation theory. In the present case of pion pair production, typical representatives are $d\sigma/d\phi_{\pi\pi}$, $d\sigma/dp_{T\,out}$. Any fixed order calculation is certainly inadequate to estimate this type of observables in the vicinity of the critical point, and, whenever possible, a Sudakov type resummation has to be carried out to restore a predictive power of the perturbative QCD calculation. As will be commented in subsect. 4.2, the colour structure of the hard subprocess in hadroproduction of pairs of hadrons is more complicated than in the celebrated case of the Drell-Yan process. This makes a soft gluon summation beyond the leading logarithmic accuracy quite sophisticated in this case. We do not provide a study of these observables based on a resummed calculation. A second family gathers observables which are less infrared sensitive than the previous ones, in the sense that their fixed order estimates do not diverge at the critical point; therefore the inadequacy of fixed order calculation to account for such observables is more difficult to foresee. Among these observables, let us mention the distribution of transverse momentum of pairs, $d\sigma/dq_T$, and the distribution $d\sigma/dZ$ where the variable Z has been defined in subsect. 3.2. They would belong to the first family, if the fragmenting partons in the final state were, instead, observed particles - as, e.g. it would be the case if they were prompt photons. In the collinear fragmentation model used here, the screening of the infrareed sensitivity stems from the convolution with fragmentation functions. this provides extra integrations over longitudinal fragmentation variables.

Computing the NLO truncation for infrared sensitive observables is more than an academic exercise. Indeed, whereas the vicinity of the critical point is infrared sensitive, the tail of the distribution may be expected safer for fixed order perturbative calculations. Yet the infrared sensitivity of these observables connects the perturbative and non perturbative regimes. At fixed target energies, depending on the observable, on the selection cuts, etc., the non perturbative effects may happen to be not confined to the vicinity of the critical point, but instead can spread over a large fraction of the physical spectrum, if not the whole. A confrontation of the NLO truncation to the measured spectrum can give a hint of the depth to which infrared, in particular non perturbative, effects penetrate a distribution away from the infrared critical point. This is what we have in mind while performing this confrontation here. Another interest concerns observables which are infrared insensitive apart from a few bins where, for example, kinematic cuts make them locally semi inclusive. The discrepancy between the NLO prediction and the measured spectrum in these bins can be related to some infrared sensitive distribution inadequately accounted for by fixed order truncation. This is typically the case with the lowest bins of the invariant mass distribution, where the discrepancy between NLO and data can be understood in the light of $d\sigma/d\phi_{\pi\pi}$, as will be explained below.

Let us add a comment about the classification which we present here, especially regarding the infrared sensitive observables. Phenomenological models are sometimes used for 'effective' k_T dependent distribution - and fragmentation - functions. For example, a popular procedure [2, 23] revisited recently [24] assumes a x independent, gaussian k_T distribution functions for on shell partons. In such a model, the behaviour of distributions such as $d\sigma/d\phi_{\pi\pi}$ and $d\sigma/dp_{T\,out}$ at respectively $\phi_{\pi\pi} \to \pi$ and $p_{T\,out} \to 0$ are smeared by the convolutions with the k_T distributions. Therefore, according to such a model, all distributions would be affected by k_T effect, i. e. the first family would be empty. In order to avoid any confusion in the terminology used, let us emphasize the following point. The models of k_T smearing mentioned above *depart* from the property of collinear factorisation, and they do not account for the higher orders corrections to the hard subprocess in perturbation theory in a consistent way. On the contrary, the classification which we present here follows closely the property of collinear factorisation which holds in perturbative QCD.

4.1 Infrared insensitive observables

Transverse momentum: one-particle inclusive vs. inclusive pair production

Let us analyse the difference between the p_T distribution of each pion in the present case of dipion production, and the p_T distribution in one particle inclusive production studied in Ref. [22]. We

have to disentangle two issues. The one concerns the difference in the ingredients used in Ref. [22] vs. the present work. It will affect the whole spectrum, and it is especially relevant in the larger p_T range. The second concerns the physics involved, and will particularly affect the lower range of the spectrum. We consider both of them successively.

First, the sets of fragmentation functions used in either case are different. This difference turns out to be quite significant in the case of single pion inclusive production. It affects the whole spectrum, and it matters especially in the higher range of the p_T spectrum, $p_T \geq 5$ GeV, where we expect perturbative QCD to apply. Indeed, as seen in Fig. 10, the u and d fragmentation functions of the KKP set are larger than the corresponding ones of the BKK set: more than 50 % above $z = 0.7$, and the ratios increase as z increases towards 1. The difference (in the same direction) is even larger for the gluon fragmentation: more than a factor 2. This is possible because the sets of fragmentation functions are extracted from data coming from e^+e^- annihilation into hadrons which constrain the fragmentation functions essentially in the range $0.1 \leq z \leq 0.7$ and because, unlike pdf's, the fragmentation functions are not tightly constrained by a momentum sum rule[11].

It is worth noticing that for p_T ranging from 4 to 10 GeV, the average value $< z >$ of the fragmentation variable z in the one particle inclusive case is $< z > \sim 0.75 - 0.90$. Therefore the theoretical estimates for single inclusive production rely on extrapolations of the fragmentation functions outside the region where they are actually constrained by the data from which they are extracted. Consequently, as emphasized in Ref. [22], the NLO predictions are plagued by a rather large uncertainty. The effect of the replacement of the BKK set by the KKP one is shown in Fig. 11. The discrepancy in normalisation between the theoretical prediction and the data is strongly reduced, for the scale choice $p_T/3$.

Comparatively, the theoretical calculation of inclusive pion pair production is less affected by the uncertainties on fragmentation functions at large z. The reason is that the values of the fragmentation variables z_1, z_2 which dominate the production of pion pairs extends in a region of smaller values than the $< z >$ in the single inclusive case, $z_{1,2}$ typically ~ 0.5, where the e^+e^- data constrain the fits of the fragmentation functions quite well. This feature is illustrated by Fig. 12. This can be traced back to the fact that the region in z, which dominates, results from a competition between the cost in energy momentum involved in the partonic subprocess – the pdf's tend to favour the smallest possible x fractions for incoming energy-momenta and therefore larger values of z – and the price to pay for a fragmentation near the end point $z = 1$ – the fragmentation stage favours small values of z. The production of a pair of two hard particles involves two fragmentation functions instead of one as in the single inclusive case, which enforces the role of fragmentation in the competition. The situation will be very different regarding the reducible background to Higgs boson search at LHC [38], because isolation requirements will select the large z region. This issue will be addressed in detail in a forthcoming article [12].

The difference in the dominant ranges of z in one particle inclusive vs. pair production sheds also some light on the apparent difference in scales which seem to be preferred by the data in either case, the optimal scale choice $\sim p_T/3$ in the one particle is apparently smaller than the choice $(3/8)\,(p_{T1} + p_{T2})$ used in pair production. Let us consider the inclusive production of a single pion in the region where the E706 data agree reasonably well with the NLO calculation using the KKP set, say, near $p_T = 6$ GeV. Such pions probe a partonic regime with a transverse momentum

[11] In the framework of independent fragmentation functions, there exists indeed a sum rule:

$$\sum_H \int_0^1 dz\, z\, D_{H/a}(z, M_f^2) = 1$$

The latter means that a parton of given species a fragments into any hadron species H with probability 1. It is however much less constraining in practice than the one holding for pdf's which relates the pdf's of all the species for a given incoming hadron.

$\sim p_T/<z>\sim 7$ GeV, and the optimal scale is ~ 2 GeV. A pair of pions, dominantly back to back, with individual $p_T \sim 3$ GeV probes a parton regime with parton transverse momenta $\sim p_T/<z_{1,2}>$ comparable with the previous one; we notice also that the scale choice used in this case is $9/4 \sim 2$ GeV. Consequently, the same partonic kinematic regime is probed in these two cases, and are found to be consistently in reasonable agreement with the same theoretical framework. We therefore conclude that the situation is actually comparable between the two cases in this p_T range. Of course this rapid investigation considers only the comparison with the data of E706. To obtain a comprehensive understanding, one needs to perform a complete study revisiting single inclusive production at fixed target energy involving other fixed targets experiments.

Let us now examine the difference in the behaviours of the p_T spectra of single inclusive production vs. each pion in pair production in the lower range of the p_T spectrum. The NLO calculations performed in the QCD improved parton model according to the property of collinear factorisation neglect non perturbative, power corrections $\sim \mathcal{O}\left(1\,\mathrm{GeV}/p_T\right)^n)$ where n depends on the observable considered. Therefore this 'leading twist' approximation is valid when $p_T \gg \mathcal{O}(1\,\mathrm{GeV})$. On the other hand, NLO calculations are not expected to predict correctly inclusive p_T spectra when p_T becomes too small, and distortions of the perturbative QCD predictions are expected up to $p_T \sim$ a few GeV. One may instead wonder why the NLO calculation and the data agree well on the slope of the distribution of each pion's p_T for pair production down to $p_T \sim p_{T\,min} = 2.5$ GeV.

Among the neglected effects, the ones induced by finite transverse momenta (k_T) of incoming partons are often assumed to be the most important. This concerns in particular the understanding of the p_T distribution at low p_T in one particle inclusive production due to the so-called 'trigger bias' effect, tentatively visualized in Fig. 13. A current practice models the latter by assuming an effective k_T distribution function[12] for the incoming partons, still considered on shell, and convolutes this with a LO calculation. If one notes $g(k_T)$ this k_T distribution, and assuming that it depends only on $|\vec{k}_T|$, one has schematically

$$\begin{aligned}\frac{d\sigma}{dp_T} &\propto \int d^2k_T\, g(k_T)\, \frac{1}{|\vec{p}_T - \vec{k}_T|^\alpha} \\ &\sim \frac{1}{p_T^\alpha}\left(1 + \frac{\alpha^2}{2}\frac{<k_T^2>}{p_T^2} + \mathcal{O}\left(\frac{<k_T^4>}{p_T^4}\right)\right)\end{aligned}$$

This means that the contribution from subprocesses initiated by partons with incoming transverse momentum pointing in the direction of the measured pion is enhanced, and this leads to an increase of the cross section in average, especially at low p_T. Let us however stress that this model is not consistent[13] with the property of collinear factorisation, established in perturbative QCD in the leading twist approximation, for inclusive processes with hard probes. Attempts of a consistent formulation have been proposed recently [25,26]. This formalism is still in an exploratory stage, and no firm and quantitative conclusions can be drawn yet.

On the other hand, the distribution of each pion's p_T in pair production involves the detection of *two* hard particles, dominantly back-to-back in the transverse plane. Therefore, any k_T kick which would

[12] For example, the popular gaussian model mentioned above.

[13] In addition it requires the use of several ad hoc extra parameters and cuts, in particular to prevent the convolution integral in eqn.(1) from diverging. The divergence of eqn. (1) when $k_T = p_T$ corresponds to a soft partonic subprocess boosted transversally by the k_T kick. The divergence obtained is an artefact of the model. Another cut-off has to be introduced to prevent the longitudinal momentum of an incoming parton a and the momentum of its parent hadron H from being in opposite directions. This nasty can occur at non zero k_T since

$$p_{a//} = \frac{1}{2}\left(x_a P_H - \frac{k_{T\,a}^2}{x_a P_H}\right)$$

where x_a is the light cone momentum fraction of H carried by a. This problem is an artefact of the modelling (an on shell parton with non zero transverse momentum and a Lorentz invariant momentum fraction). See [23] for a review.

favour one pion in a pair would penalize the other [2]. This is tentatively pictured by the top drawing in Fig. 14. In particular, in the lower range of the p_T spectrum, the p_T of the penalized pion may even be pulled down below the selection cut $p_{T\,min}$ so that the event may be discarded, cf. bottom drawing in Fig. 14. Consequently, when the selection cut is symmetric, the mentionned trigger bias is reduced. If the mechanism of k_T gives the dominant power correction in the single inclusive p_T spectrum at low p_T, its lesser influence on the p_T spectrum of each pion in pair production allows perturbative QCD to extend its range of validity down to fairly low p_T values. Let us notice that the absence of trigger bias effects is expected as well if, instead of the distribution of each pion's p_T, but with the same selection cuts, one would consider the p_T distribution of the 'leading' pion (the one with the largest p_T in the pair), even though the latter seemingly displays the p_T of only one particle. On the other hand, an interpolating case would be the distribution of each pion's p_T in pair production when the selection cuts on the two pions are asymmetric. The behaviour of the distribution of each pion's p_T is expected to exhibit the same trigger bias effect as the single inclusive case when the p_T cut on the second pion becomes very low.

The invariant mass distribution of pairs, $d\sigma/dm_{\pi\pi}$

The *DIPHOX* calculation and the E706 data agree reasonably well on this observable for $m_{\pi\pi} \geq 5.0$ GeV. On the other hand we see a sharp disagreement on the first two bins in invariant mass. In this respect we notice that

$$m_{\pi\pi} = \sqrt{2p_{T1}\,p_{T2}(\cosh(2y^*) - \cos\phi_{\pi\pi})} \tag{1}$$

$\phi_{\pi\pi}$ being the azimuthal angle between the two pions. At LO, the $2 \to 2$ kinematics forces the p_T of the two pions to be back-to-back ($\cos\phi_{\pi\pi} = -1$) and the value 5 GeV, which corresponds to 2 $p_{T\,min}$, is the minimal value which can be taken by $m_{\pi\pi}$ at LO. In other words, the first two bins of the theoretical calculation are filled only by NLO, inelastic contributions, for which $\phi_{\pi\pi} < \pi$. The sharp disagreement between the NLO calculation and the data in these two bins is therefore correlated with the situation regarding the distribution in azimuthal angle difference between the two pions in a pair, which will be examined in sect. 4.2.

The distribution $d\sigma/d\cos\theta^*$

As seen on Fig. 5, the measured distribution $d\sigma/d\cos\theta^*$ and the corresponding NLO distribution show a fairly good agreement in shape but an overall discrepancy in normalisation[14], the theoretical prediction being systematically above the data by a constant multiplicative factor ~ 1.4 for the scale choice used. One may wonder why, for the given scale choice in the NLO calculation, and for the same data sample, the agreement in normalisation seems somewhat worse for this distribution than what is found in average for the other infrared insensitive distributions.

Firstly, it should be stressed that this $\cos\theta^*$ distribution is much more tricky than its naming suggests. Indeed, the distribution shown in Fig. 5 is *not* literally the bare quantity $d\sigma/d\cos\theta^*$. Let us recall that the 'naive, bare' distribution $d\sigma/d\cos\theta^*$, without additional cut, has a bell-like shape peaked at $y^* = 0$ and decreasing towards 0 as $|y^*|$ is increasing. This results from a competition between the behaviour of the partonic matrix element squared, and the fall-off of the pdf's when $x \to 1$. The matrix element squared behaves as as $(1 \pm \cos\theta^*)^{-\alpha}$ when $\cos\theta^*$ increases, in the case of a massless spin s exchange in the t or u channel: a distribution unveiling this behaviour would namely probe the short distance dynamics. On the other hand $x_i \to 1$ for $i = 1$ or 2 when $|y^*|$ increases[15], and this effect wins. Additional cuts are implemented to freeze the influence of the pdf's

[14] A current presentation of this observable normalises the measured distribution and the NLO prediction separately in such a way that the bin content corresponding to $\cos\theta^* = 0$ is equal to 1. The discrepancy in normalisation is therefore hidden by this procedure.

[15] See for instance [23] for explicit LO expressions.

and magnify the short distance dynamics. The additional cuts restrict the data sample providing this $\cos\theta^*$ distribution: this sample is *not* the same as the one yielding the other infrared insensitive distributions, but only a subsample of it. In particular, an auxiliary selection cut on the invariant mass $m_{\pi\pi} \geq 7$ GeV is imposed, in order to avoid p_T-threshold effects induced by the selection cut $p_T > p_{T\,min}$ [1]. The whole distribution carved out this way is dominated by the pairs with $m_{\pi\pi} \sim 7.0 - 8.0$ GeV. We then notice on Fig. 3 for the invariant mass distribution that the ratio data/NLO in the corresponding bins is approximately 0.7, a value consistent with what is observed on Fig. 5 bottom for the $\cos\theta^*$ distribution. In summary the normalisation of the whole $\cos\theta^*$ distribution is given by the one of only a few bins of the $m_{\pi\pi}$ distribution. This makes the overall normalisation in the NLO $\cos\theta^*$ distribution very much scale dependent. If, instead of choosing the scale 'preferred' by the each pion's p_T distribution in the theoretical calculation as explained in sect. 3, we take a scale which makes the ratio Data/Theory close to 1 for the $m_{\pi\pi}$ distribution, this apparent normalisation problem disappears.

4.2 Infrared sensitive observables

We now successively examine the two families of infrared sensitive observables which we identified at the beginning of this section. We first focus on the distribution $d\sigma/d\phi_{\pi\pi}$ as an example of observables with strong infrared sensitivity. Next we consider the cases of the q_T and Z distributions, as examples of observables for which the infrared sensitivity is smeared. Later we examine how the sensitivity of these types of observables to non perturbative effects evolves with increasing individual transverse momenta of the pions and/or with increasing invariant masses of the pairs.

The angular distribution $d\sigma/d\phi_{\pi\pi}$

As can be seen on Fig. 6, the 'NLO distribution' and the experimental spectrum are absolutely different. The LO contribution to the 'NLO distribution' is proportional to $\delta(\pi - \phi_{\pi\pi})$, and the inelastic part of its NLO contribution diverges as $\mathcal{O}(\alpha_s \ln(\pi - \phi_{\pi\pi})/(\pi - \phi_{\pi\pi}))$ when $\phi_{\pi\pi} \to \pi$. Therefore the 'NLO distribution' is mainly concentrated in the last bin containing $\phi_{\pi\pi} = \pi$ at the elastic boundary of the spectrum. In contrast the experimental distribution is spread out much more and flatter. The discrepancy is so spectacular that one has to ask the question, why there is such a satisfactory agreement for the p_T distribution, cf. Fig. 2, and, similarly what the reason is for the sharp disagreement in the first two bins for the invariant mass distribution in Fig. 3, while the agreement is satisfactory in the other bins.

We notice that, although the shapes of the 'NLO distribution' and of the measured distribution are completely different, the area below these distributions are approximately equal. This suggests that long distance phenomena, which are ignored in the NLO calculation, proceed to nothing but a drastic kinematic 'reshuffle' of the configurations of the hard partons involved in the subprocess into the ones of the measured pions, i.e. a probabilistic redistribution of kinematic variables occurring with total probability 1. This hypothesis is supported by the following argument. Looking back to the invariant mass distribution of pairs, we noticed previously a strong disagreement between the NLO prediction and the data in the first two bins. Quantitatively, the theoretical result is more than a factor 25 smaller than the measured central value for the second bin 4.5 GeV $\leq m_{\pi\pi} \leq$ 5.0 GeV, and it is about a factor 60 smaller in the first bin 4.0 GeV $\leq m_{\pi\pi} \leq$ 4.5 GeV. Given the fast fall-off of the p_T distribution the pion pairs for which the individual pions' p_T are minimal i.e. close to 2.5 GeV both dominate the first bins of the invariant mass distribution, and control the $\phi_{\pi\pi}$ distribution. Furthermore, pairs with small y^* dominate. Therefore, approximating the identity (1) by roughly $m_{\pi\pi} \sim 2p_{T\,min}\sin(\phi_{\pi\pi}/2)$ we infer that the first and second bins in invariant mass are dominated by pairs with respectively $\phi_{\pi\pi} \sim 115^{\,o}$ and $\phi_{\pi\pi} \sim 140^{\,o}$. If we now look at the discrepancy between the 'NLO calculation' and the measured distribution for the $\phi_{\pi\pi}$ spectrum at these values of $\phi_{\pi\pi}$, we find respectively ~ 40 and 20. These values are comparable with the ones for the discrepancies

between NLO results and data for the invariant mass spectrum in the corresponding first and second bin in invariant mass.

A proper understanding of the shape of the distribution $d\sigma/d\phi_{\pi\pi}$ requires the all order summation of the large Sudakov logarithms which appear order by order in the theoretical calculation. The latter come from soft gluon emission in both initial and final states - and, beyond leading logarithmic accuracy, from interferences between them. The colour structure involved [27, 28] is quite more intricate than in the well-known processes of Drell-Yan [29–32] and nearly back-to-back hadron production in hadronic e^+e^- annihilation [33]. This summation has not been performed yet for the $\phi_{\pi\pi}$ distribution. Beyond this summation, non perturbative effects are also involved. In the analysis of infrared sensitive distributions of electrodynamic probes in fixed targets experiments, such as the transverse momentum distribution of lepton pairs in Drell-Yan or of photon pairs in prompt photon pairs production [34], such non perturbative effects have been shown to be important over a large fraction of the spectrum. In the present case they may have even larger effects. They may come in particular from some k_T kick on initial partons, as well as on the hadrons produced by the fragmentation process. Since both the initial and final states are affected by these phenomena, and since the selection cut on the p_T of the pions is not much larger than the typical scale $\sim \mathcal{O}(1\text{ GeV})$ of non perturbative phenomena in strong interaction, even a rather moderate effective k_T kick - several hundreds of MeV 'per hard coloured leg' - may be able to reshuffle the hard parton configuration drastically, as one can convince oneself with the cartoon drawn in Fig. 15.

It is important to understand how it is conceivable that the infrared insensitive observables can be reasonably estimated using perturbative, fixed order calculations, whereas there exist distributions, such as $d\sigma/d\phi_{\pi\pi}$ which are so heavily distorted by non perturbative effects. The key point is the following: if this probabilistic reshuffle acts on kinematic variables which are integrated over during the calculation of some distribution, and if the available phase space for this kinematic variable is not severely amputated by some selection cut in the range considered, this reshuffling leaves nearly no fingerprint in this observable. This seems to be what happens for the distribution of each photon's p_T (the variable $\phi_{\pi\pi}$ is integrated out when the $\vec{p}_T$ of the other photon is integrated out). The same conclusion holds also, for example, for the invariant mass distribution as soon as the invariant mass is large enough compared to $2\,p_{T\,min}$. It does not hold when $m_{\pi\pi}$ is near or below this value because of the restriction acting on $\phi_{\pi\pi}$ through eqn.(1).

Transverse momentum distribution of pairs, $d\sigma/dq_T$

As we mentioned in the general introduction of this section, the situation in the case at hand is different from the one usually faced concerning this observable in the Drell-Yan process/production of a weak vector boson, or in the production of pairs of prompt photons[16]. E.g., in the Drell-Yan case, the calculation of this distribution is singular at $q_T = 0$ order by order in perturbation theory. In particular the zeroth order contribution to $d\sigma/dq_T^2$ is proportional to $\delta(q_T^2)$ by transverse momentum conservation, and logarithmically enhanced '+' distributions are involved at every successive order. On the contrary, in the present case, the double convolution with the two fragmentation functions makes the calculation finite at every transverse momentum q_T of the pair, order by order in perturbation theory. In particular it is non vanishing already at lowest order for every $q_T > 0$ allowed by kinematics. One may therefore expect a somewhat reduced infrared sensitivity, compared with the $\phi_{\pi\pi}$ distribution. The comparison between the NLO calculation and the measured q_T distribution, cf. Fig. 8, namely the examination of the discrepancy between the former and the latter suggest that it is hardly the case. Whereas the discrepancy reaches quantitatively a magnitude of 20 to 50 in the $\phi_{\pi\pi}$ case, it is 'only' about a factor 5 to 10 for the q_T distribution. Moreover the

[16] More precisely, we mean here the production of photon pairs through the so-called 'direct' mechanism, cf. sect. 2 and Ref. [13]. On the contrary the production of pairs of 'photons from fragmentation' is very similar to the present case.

NLO calculation is still inadequate in shape as well over all the measured q_T. This inadequacy is related to the discrepancy in the $\phi_{\pi\pi}$ distribution examined in the previous subsection. Let us write $q_T^2 = (p_{T1} - p_{T2})^2 + 2p_{T1}p_{T2}(1 + \cos\phi_{\pi\pi})$. The $\phi_{\pi\pi}$ distribution is concentrated in the vicinity of $\phi_{\pi\pi} = \pi$ whereas the experimental one is more flat and spread. Therefore the NLO result for the q_T is peaked near $q_T = 0$ and is higher than the experimental spectrum in this region. As for configurations with a larger q_T, they can have two origins. Either the individual p_T's have to be larger, but NLO and data agree on the p_T distribution, hence this origin contributes by the same amount to the NLO result and to the data; or $\phi_{\pi\pi}$ is far from π, in which case the NLO $\phi_{\pi\pi}$ distribution is much below the experimental one. This makes the NLO q_T distribution fall faster than the measured one as q_T gets larger.

Transverse momentum balance distribution $d\sigma/dZ$

This observable is another case of distribution which is singular e.g. in diphoton production, namely at the critical point $Z = 1$. Indeed, in diphoton production, the contribution of the 'direct' mechanism is proportional to $\delta(1-Z)$ at lowest order by transverse momentum conservation, and involves logarithmic singularities at every higher order. Due to the same reason as in the previous example, this distribution is, instead, finite for all Z, order by order in perturbation theory. As can be seen on Fig. 9, the comparison between the NLO calculation and the experimental distribution roughly agrees for $Z > 1$, but is inadequate for $Z < 1$. This can be understood as follows. From $Z = -p_{T1}/p_{T2}\cos\phi_{\pi\pi}$ one sees that $p_{T1} > p_{T2}$ is a necessary condition to have $Z > 1$. Since this occurs preferably with values of $\phi_{\pi\pi}$ not far from π, one understands that the NLO curve overshoots the data slightly regarding the last bins of the $\phi_{\pi\pi}$ distribution, cf. Fig. 6. Yet the reversal of the ordering of the respective magnitudes of the NLO and measured $\phi_{\pi\pi}$ distributions occurs for a value $\phi_{\pi\pi}$ close to π. The integration over the fragmentation variables averages these two opposite orderings, and makes the discrepancy between the NLO and measured Z distribution rather small for $Z > 1$. On the other hand, for $Z < 1$, p_{T1} and p_{T2} are unconstrained and most likely of comparable size. This Z region thus selects the lower range of $\cos\phi_{\pi\pi}$ and for small Z one finds a similar large discrepancy as for the $\phi_{\pi\pi}$ distribution in the lower $\phi_{\pi\pi}$ range.

4.3 Energy dependence of the non perturbative effects

The sensitivity of the infrared sensitive observables examined above to non perturbative aspects is strong and extended to a large fraction, if not the totality, of the measured spectrum. This is mainly because the E706 data were selected above a cut $p_{T\,min} \geq 2.5$ GeV, and because the normalisations and shapes of these distributions are dominated by the pairs in which the individual p_T's of the pions are close to $p_{T\,min}$, a value not large with respect to the typical scale of non perturbative effects. As we are interested in making predictions for collider experiments, especially for the LHC [12], it would be interesting to see how the situation evolves with the scales. Two situations have to be distinguished: 1) the increase of the 'hard scale', loosely speaking – i.e. the invariant mass of the pair, or the individual p_T's of the pions in pairs – at fixed $\sqrt{S}$, and 2) the increase of $\sqrt{S}$ at fixed 'hard scale'.

In the archetype of the Drell-Yan process, for the distribution $d\sigma/dq_T dm$ of lepton pairs, this question has been studied relying on resummed calculations. In particular, the authors of Refs. [30, 32] have studied how the sensitivity to non perturbative effects at $q_T = 0$ evolves as a function of m. They determined which region dominates the Sudakov-type factor in impact parameter (b) space, by mean of a saddle point analysis. They showed that the dominant region in b space is purely non perturbative at m values in the fixed target energy range, but that it migrates towards smaller values of b and ultimately fits completely inside the perturbative region $\Lambda_{QCD}b \ll 1$ when m becomes large enough. This indicates that the non perturbative effects become confined to a closer and closer vicinity of the critical point as the invariant mass m increases. This feature makes it difficult to

extract a precise parametrisation of these non perturbative effects from experimental data [35–37]. On the other hand it implies that theoretical predictions at higher, collider energies are less affected.

In this subsection, we perform a phenomenological study through which we try to extract information about item 1) within the range covered by the E706 experiment. As noticed in the last two subsections, the $\phi_{\pi\pi}$ distribution is the key of the understanding of the others. A useful information could be extracted from data samples ordered according to increasing values of $p_{T\,min}$ for fixed $\sqrt{S}$. Tabulations of data of this type are available for the invariant mass distribution. However not much information can be learned from it since this observable is blind to non perturbative effects over most of its spectrum. On the other hand, such tabulations are not available for the more instructive $\phi_{\pi\pi}$ distribution. An alternative could be provided by a refined double binning of the data according to the infrared sensitive variable considered and, simultaneously, to increasing invariant mass, the latter corresponding loosely to increasing individual p_T's of each pion in pairs. This type of double binning is available for the $p_{T\,out}$ distribution, but again not for the $\phi_{\pi\pi}$ distribution. The only information available about $\phi_{\pi\pi}$ in this respect is the average $<\phi_{\pi\pi}>$ [1].

Increasing the hard scale at fixed $\sqrt{S}$.

Let us thus consider the average values of the azimuthal angle difference between the two pions of pairs, $<\phi_{\pi\pi}>$ as a function of the invariant mass of the pair. Of course the shape of the $\phi_{\pi\pi}$ distribution is infrared sensitive near $\phi_{\pi\pi} = \pi$ and, to any fixed order in perturbation theory, the theoretical estimate of the $\phi_{\pi\pi}$ distribution is divergent at $\phi_{\pi\pi} = \pi$. However when the average $<\phi_{\pi\pi}>$ is computed, the Sudakov logarithms are smeared out by the integration order by order in perturbation theory. There is no logarithmic enhancement in $<\phi_{\pi\pi}>$ order by order in perturbation theory anymore. Consequently, a fixed order calculation of $<\phi_{\pi\pi}>$ is expected to become more and more accurate for harder and harder pion pairs, without a detailed knowledge of the shape. Non perturbative effects are expected to induce deviations in the form of power corrections $\mathcal{O}\,(1\,\mathrm{GeV}/p_T)$, $\mathcal{O}\,(1\,\mathrm{GeV}/m_{\pi\pi})$.

For $m_{\pi\pi} > 5$ GeV, the full range $105^o \leq \phi \leq 180^o$ is accessible[17], and $<\phi_{\pi\pi}>$ is dominated by the nearly back-to-back region. This dominance of the region $\phi_{\pi\pi} \sim \pi$ is actually stronger in the NLO result than in the data. Indeed, the pairs of pions with low individual p_T and relatively low invariant mass dominate the $\phi_{\pi\pi}$ distribution discussed in subsect. 4.2. The latter is thus strongly sensitive to non perturbative effects, which make it much flatter than the shape of the NLO result. Therefore the experimental values of $<\phi_{\pi\pi}>$ should be lower than the NLO values. The distribution $d\sigma/dm_{\pi\pi}d\phi_{\pi\pi}$ should then become steeper and more concentrated near the back-to-back region with increasing invariant mass, if non perturbative effects become less and less important. The experimental values of $<\phi_{\pi\pi}>$ should increase with increasing invariant mass, and the difference between them and the corresponding NLO results should decrease. The general trend of the data seem to agree with this expectation, as suggested by Fig. 16. To be fair however, the very large error bars prevent from drawing any firm conclusion. More generally, the first moment of infrared sensitive distribution is not sensitive enough to long distance effects. Cumulants of higher orders of these distributions would be much more instructive in this respect, not speaking about these distributions themselves.

We examined also the distribution $d\sigma/dp_{T\,out}dm_{\pi\pi}$ sliced in broad bins of invariant mass. As seen on Fig. 17 all plots for each separate bin of invariant mass are similar to the one shown in Fig. 7. The NLO result is inadequate to account for the measured distribution for all invariant masses, and nothing instructive can be extracted from it regarding the range of influence of non perturbative

[17]The situation in the first bins with $m_{\pi\pi} \leq 5$ GeV is peculiar. In these bins the selection cut $p_T > p_{T\,min}$ forbids the back-to-back region as discussed previously. The average $<\phi_{\pi\pi}>$ is thus much smaller than π. This holds both for the NLO result and the data, and no relevant information can be extracted regarding the problem concerned by this discussion.

effects with respect to the invariant mass. Last, in the case of the distribution $d\sigma/dZdm_{\pi\pi}$, we notice on Fig. 18 that the discrepancy between the NLO result and the data for $Z < 1$ decreases with increasing $m_{\pi\pi}$. This holds at least for Z values not very small with respect to 1, for bins in invariant mass which gather enough statistics so that any conclusion can be drawn.

It would have been interesting also to identify how the magnitude of non perturbative effects evolves when the beam energy increases from 530 to 800 GeV. Unfortunately, the level arm in $\sqrt{S}$ is too small and the errors bars are too large to extract this information.

5 Conclusions and outlook

We have compared NLO predictions with data of the E706 experiment for various observables. We have classified the observables according to their respective infrared sensitivity. For the class of infrared insensitive observables the NLO predictions agree rather well with the corresponding measured ones over the whole measured spectrum. In contrast, the NLO result is inadequate to describe infrared sensitive observables, not only in the close vicinity of the infrared sensitive region as expected, but even over a large fraction of, if not the whole spectrum. The phenomenological analysis performed in this article suggests that the discrepancy can be understood in terms of a probabilistic reshuffle of the partonic configurations involved in the NLO calculation. From a theoretical point of view a Sudakov-type summation of logarithmically enhanced infrared terms which appear order by order in perturbation theory in the expansion of these infrared sensitive observables is mandatory. Yet it is likely to be not enough, as the discrepancy is probably dominated by large non perturbative effects. The non perturbative dynamics strongly distorts the infrared sensitive observables because the experimental selection cut $p_{T\,min}$ imposed on each pion is not large compared to the typical non perturbative scale $\mathcal{O}(1)$ GeV. On the other hand, these non perturbative effects turn out to be weak on infrared insensitive distributions. In particular they are much weaker than in the case of one particle inclusive production, especially on the p_T distribution in the lower p_T range. This can be traced back to the absence of trigger bias in pair production when symmetric cuts are applied, contrarily to the situation in one particle production. A further examination of the E706 data tends to suggest that these non perturbative effects become less and less important in the infrared sensitive distributions, and in particular more and more confined to the vicinity of the critical points, as the p_T's of the selected pions increase for fixed $\sqrt{S}$, although, to be fair, no definite conclusion can be extracted from this examination due to large experimental uncertainties. On the other hand no evolution of the magnitude of non perturbative effects can be seen when going from 530 to 800 GeV because the level arm in $\sqrt{S}$ is not large enough.

We expect these features to hold as we move from fixed target to collider experiments, as soon as the selection cut $p_{T\,min}$ increases up to 10-15 GeV at the Fermilab Tevatron and 20-40 GeV at the forthcoming LHC. We therefore expect NLO predictions to be reliable in particular for inclusive observables concerning pions pairs - as well as $\gamma\pi^0$ pairs - at the Tevatron and LHC, at least far enough from the boundaries of the spectrum. On the other hand, near these boundaries, the various kinematic cuts can induce extra infrared sensitivity in partonic calculations. This is certainly expected to hold for observables which do not require any isolation cut. On the other hand, the implementation of isolation can affect the ability of fixed order perturbative calculations to provide reliable predictions for most inclusive distributions. This problem, which is of particular relevance in the calculation of backgrounds to the Higgs boson search at LHC in the channel $H \to \gamma\gamma$, will be examined in detail in a forthcoming article [38].

Acknowledgments. We wish to thank M. Zelinski for several useful discussions and M. Begel for correspondence. We thank also M. Fontannaz for relevant remarks in the comparison between one particle inclusive and pair production. This work was supported in part by the EU Fourth Training Programme "Training and Mobility of Researchers", Network "Quantum Chromodynamics and the

Deep Structure of Elementary Particles", contract FMRX-CT98-0194 (DG 12 - MIHT). LAPTH is a "Unité Mixte de Recherche (UMR 5108) du CNRS associée à l'Université de Savoie".

Note added. During the completion of this article, we became aware of a recently submitted article by J.F. Owens [39] also dedicated to dihadron production.

References

[1] E706 Collaboration, L. Apanasevich *et al.*, *Phys. Rev. Lett.* **81** (1998) 2642;
M. Begel, Production of High Mass pairs of Direct Photons and Neutral Mesons in a Tevatron Fixed-Target Experiment, Ph.D. Thesis, Rochester University, NY, 1999 - hep-ex/9711017.

[2] R. Baier, J. Engels and B. Peterson, *Z Phys.* **C2** (1979) 265.

[3] J. Bienewiess, B.A. Kniehl and G. Kramer, *Phys. Rev.* **D53** (1996) 6110.

[4] B.A. Kniehl, G. Kramer and B. Pötter, *Nucl. Phys.* **B582** (2000) 514.

[5] B.A. Kniehl, G. Kramer and B. Pötter, *Nucl. Phys.* **B597** (2001) 337.

[6] CDF Collaboration, F. Abe *et al.*, *Phys. Rev. Lett.* **73** (1994) 2662; Erratum-ibid.**74** (1995) 1891.

[7] D0 Collaboration, B. Abbott *et al.*, *Phys. Rev. Lett.* **84** (2000) 2786.

[8] ATLAS Technical proposal, CERN/LHCC 94-43; ATLAS detector and physics performance TDR, CERN/LHCC 99-14.

[9] CMS Technical proposal, CERN/LHCC 94-38; CMS ECAL TDR CERN/LHCC 97-33.

[10] The ATLAS and CMS Collaboration, ed. by J.G. Branson, D. Denegri, I. Hincliffe, F. Gianotti, F.E. Paige and P.Sphicas, preprint BNL-HET-01-33 - hep-ph/0110021.

[11] S. Catani *et al.*, in Proc. CERN Workshop on Standard Model Physics (and more) at the LHC, Geneva 1999, ed. by G. Altarelli and M. Mangano, 1-113 CERN-TH-2000-131 - hep-ph/0005025.

[12] T. Binoth, Talk given at 36th Rencontres de Moriond on QCD and Hadronic Interactions, Les Arcs, France, 17-24 March 2001, hep-ph/0105149.

[13] T. Binoth, J.Ph. Guillet, E. Pilon, M. Werlen, *Eur. Phys. J.* **C16** (2000) 311.

[14] T. Binoth, J.Ph. Guillet, E. Pilon, M. Werlen, *Phys. Rev.* **D63** (2001) 114016.

[15] T. Binoth, Talk given at 35th Rencontres de Moriond on QCD and Hadronic Interactions, Les Arcs, France, March 2000, hep-ph/0005194.

[16] S. Catani, J.-P. Guillet, M. Fontannaz and E. Pilon, in preparation.

[17] CCOR Collaboration, A.l.S. Angelis *et al*, *Nucl.Phys.* **B209** (1982) 284.

[18] NA24 Collaboration, C.D. Marzo *et al*, *Phys. Rev.* **D42** (1990) 748.

[19] CTEQ Collaboration, H.L. Lai *et al.*, *Eur. Phys. J.* **C12** (2000) 375.

[20] P.M. Stevenson, *Phys. Rev.* **D23** (1981) 2916.

[21] P. Aurenche, R. Baier, M. Fontannaz and D. Schiff, *Nucl. Phys.* **B286** (1987) 509.

[22] P. Aurenche, M. Fontannaz, J.P. Guillet, B. Kniehl and M. Werlen, *Eur. Phys. J.* **C13** (1999) 347.

[23] J.F. Owens, *Rev. Mod. Phys.* **59** (1987) 465.

[24] L. Apanasevich *et al.*, *Phys. Rev.* **D59** (1999) 074007.

[25] H.-L. Lai and H.-N. Li, *Phys.Rev.* **D58** (1998) 114020

[26] E. Laenen, G. Sterman and W. Vogelsang, *Phys. Rev. Lett.* **84** (2000) 4296; ibid., *Phys. Rev.* **D63** (2001) 114018.

[27] R. Bonciani, S. Catani, M. Mangano, P. Nason, *Nucl. Phys.* **B529** (1998) 424

[28] N. Kidonakis, G. Oderda and and G. Sterman, *Nucl. Phys.* **B531** (1998) 365

[29] Yu.L. Dokshitzer, D. Diakonov and S.I. Troyan, *Phys. Rep.* **58** (1980) 269.

[30] G. Parisi and R. Petronzio, *Nucl. Phys.* **B154** (1979) 427.

[31] A. Bassetto, M. Ciafaloni, G. Marchesini, *Phys.Rep.* **100** (1983) 201.

[32] J.C. Collins, D.E. Soper and G. Sterman, *Nucl.Phys.* **B250** (1985) 199.

[33] J.C. Collins, D.E. Soper, *Nucl.Phys.* **B193** (1981) 381; ibid, *Nucl.Phys.* **B197** (1982) 446.

[34] P. Chiappetta, R. Fergani and J.-P. Guillet, *Phys. Lett.* **B348** (1995) 646.

[35] C. Davies, B.R. Webber and W.J. Stirling, *Nucl.Phys.* **B256** (1985) 413.

[36] G.A. Ladinsky and C.-P. Yuan, *Phys. Rev.* **D50** (1994) 4239.

[37] R.K. Ellis, D.A. Ross and S. Veseli, *Nucl. Phys.* **B503** (1997) 309.

[38] T. Binoth, J.Ph. Guillet, E. Pilon, M. Werlen, article in preparation.

[39] J.F. Owens, hep-ph/0110036.

Figures

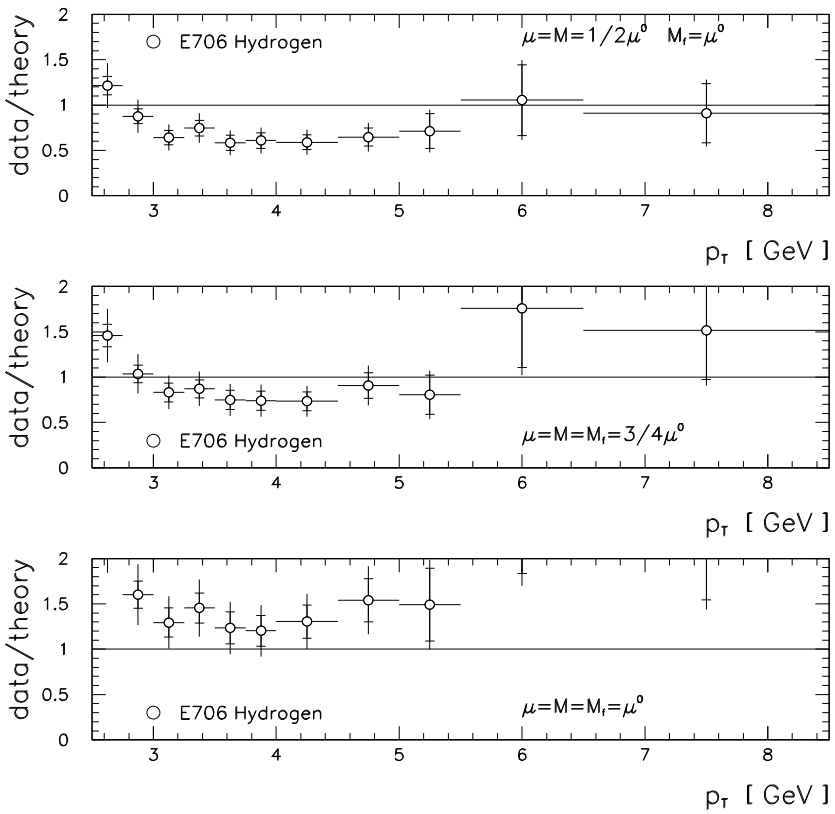

Figure 1: Scale dependence of the NLO prediction for the p_T distribution in 800 GeV proton collisions on H target, $\mu^0 = (p_{T1} + p_{T2})/2$.

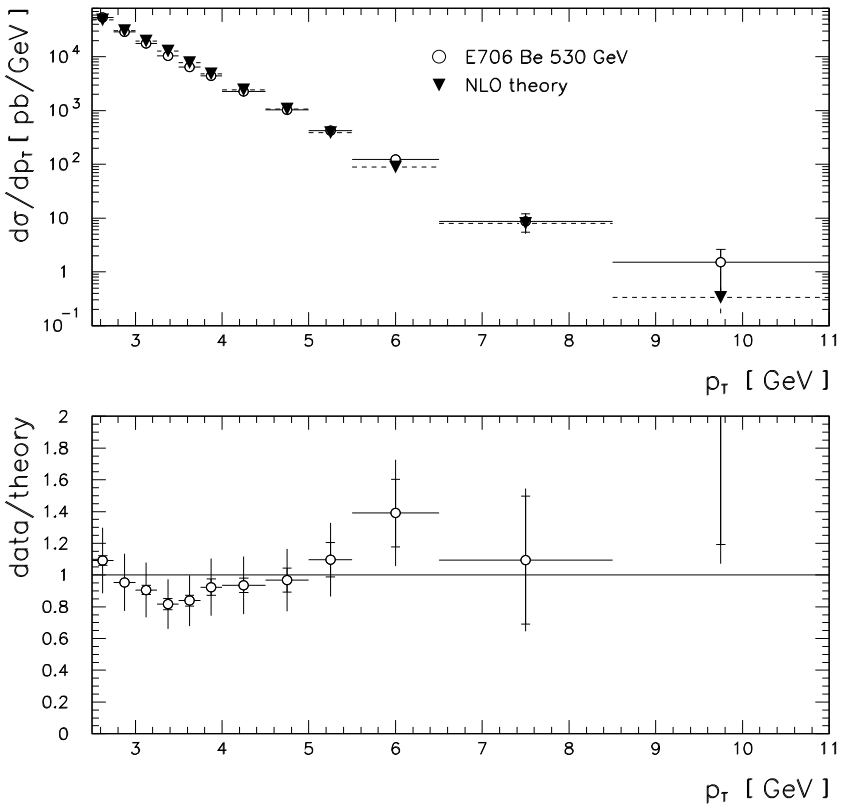

Figure 2: Dipion differential cross section $d\sigma/dp_T$ vs. p_T, the transverse energy of each pion, in $p - Be$ collisions with a beam energy of 530 GeV. Data points with statistical and systematic errors in quadrature are from the E706 collaboration [1]. The NLO prediction with scales $M = \mu = M_f = 3/8\,(p_{T1} + p_{T2})$ is shown as triangles.

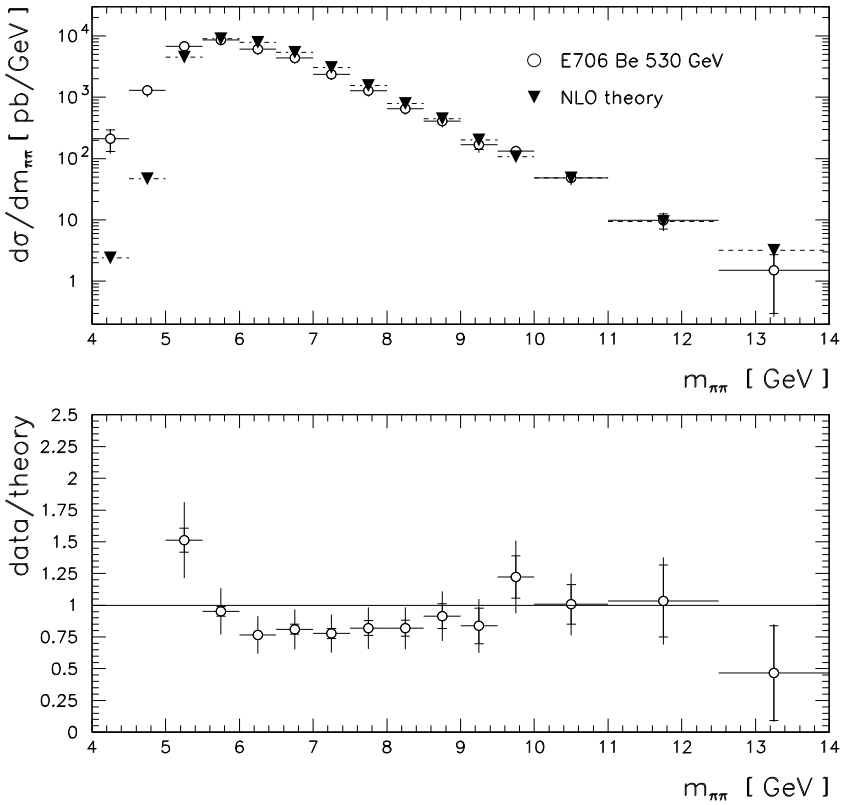

Figure 3: Dipion differential cross section $d\sigma/dm_{\pi\pi}$ vs. $m_{\pi\pi}$, the invariant mass of the pair, in $p-Be$ collisions with a beam energy of 530 GeV. Data points with statistical and systematic errors in quadrature are from the E706 collaboration [1]. The NLO prediction with scales $M = \mu = M_f = 3/8\,(p_{T1} + p_{T2})$ is shown as triangles. With the chosen ordinate scale in the bottom histogram, the first two points fall outside the plot.

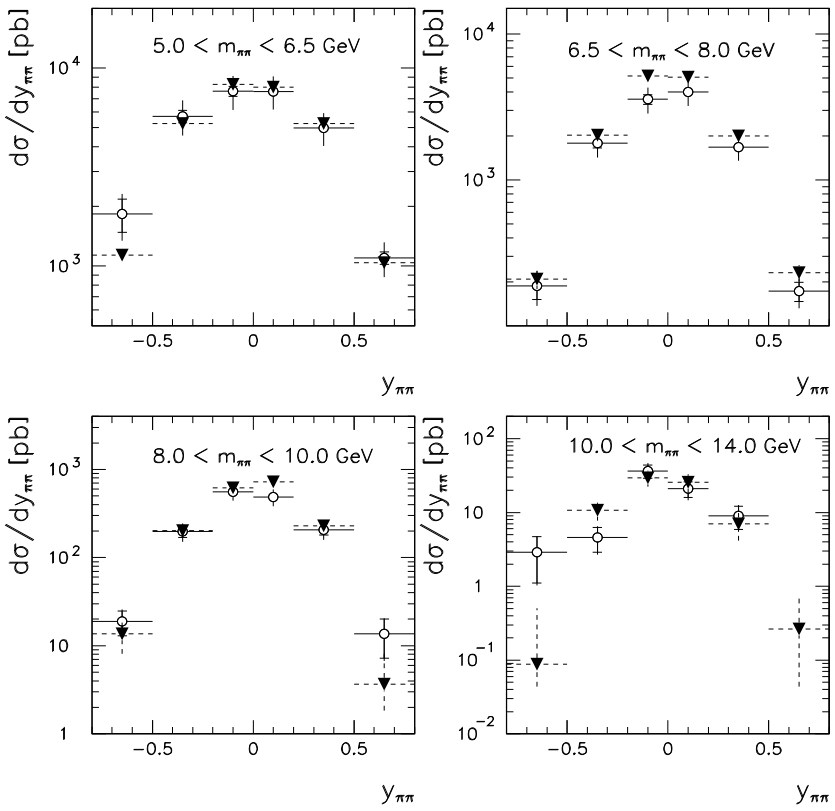

Figure 4: Dipion differential cross section $d\sigma/dy_{\pi\pi}$ vs. $y_{\pi\pi}$, the rapidity of the pair in $p-Be$ collisions with a beam energy of 530 GeV. Here $d\sigma/dy_{\pi\pi}$ stands for $\int dm_{\pi\pi}(d\sigma/dy_{\pi\pi}dm_{\pi\pi})$ integrated over the following invariant mass slices: $5.0 < m_{\pi\pi} < 6.5$ GeV (top left), $6.5 < m_{\pi\pi} < 6.5$ GeV (top right), $8.0 < m_{\pi\pi} < 10.0$ GeV (bottom left) and $10.0 < m_{\pi\pi} < 14.0$ GeV (bottom right). Data points with statistical and systematic errors in quadrature are from the E706 collaboration [1]. The NLO prediction with scales $M = \mu = M_f = 3/8\,(p_{T1} + p_{T2})$ is shown as triangles.

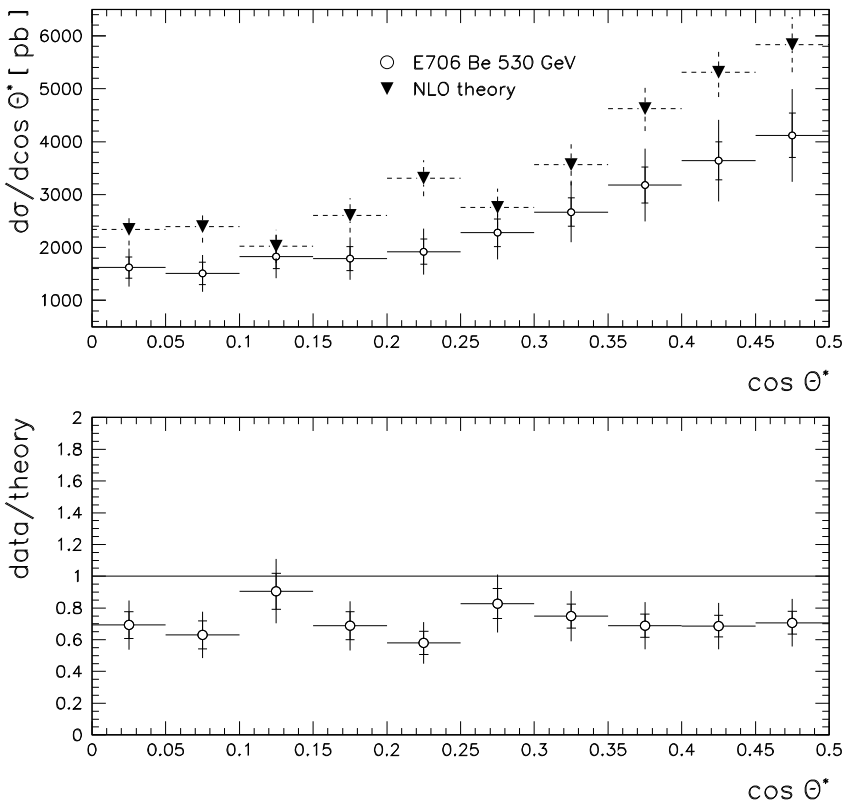

Figure 5: Dipion differential cross section $d\sigma/d\cos\theta^*$ vs. the variable $\cos\theta^*$ defined in subsect. 3.1, in $p-Be$ collisions with a beam energy of 530 GeV. Data points with statistical and systematic errors in quadrature are from the E706 collaboration [1]. The NLO prediction with scales $M = \mu = M_f = 3/8\,(p_{T1} + p_{T2})$ is shown as triangles.

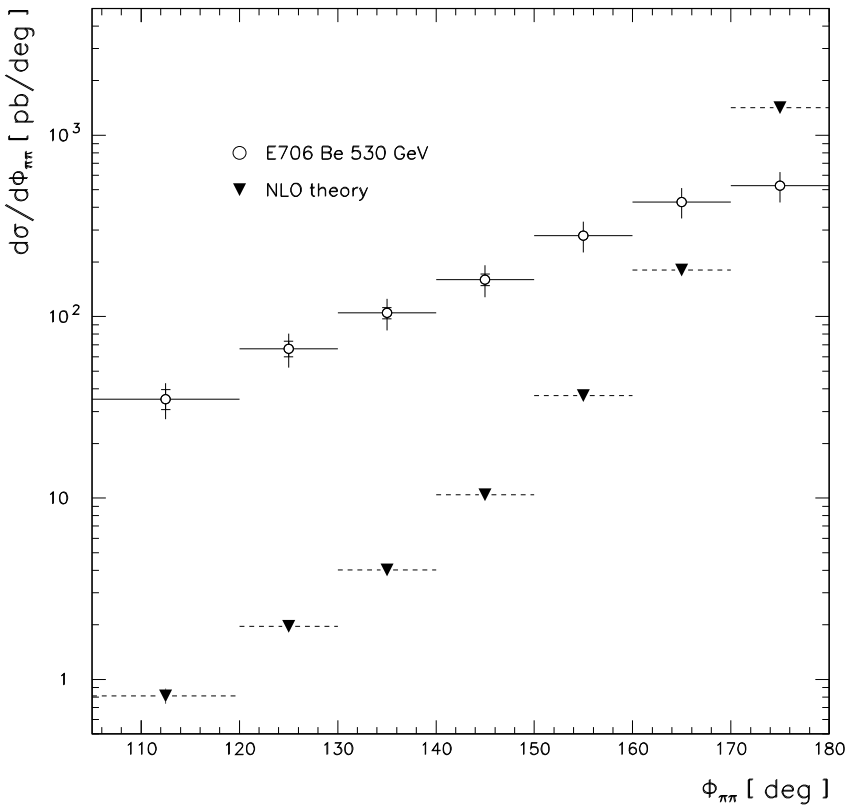

Figure 6: Dipion differential cross section $d\sigma/d\phi_{\pi\pi}$ vs. $\phi_{\pi\pi}$, the azimuthal angle difference between the two pions in a pair, in $p-Be$ collisions with a beam energy of 530 GeV. Data points with statistical and systematic errors in quadrature are from the E706 collaboration [1]. The NLO prediction with scales $M=\mu=M_f=3/8\,(p_{T1}+p_{T2})$ is shown as triangles.

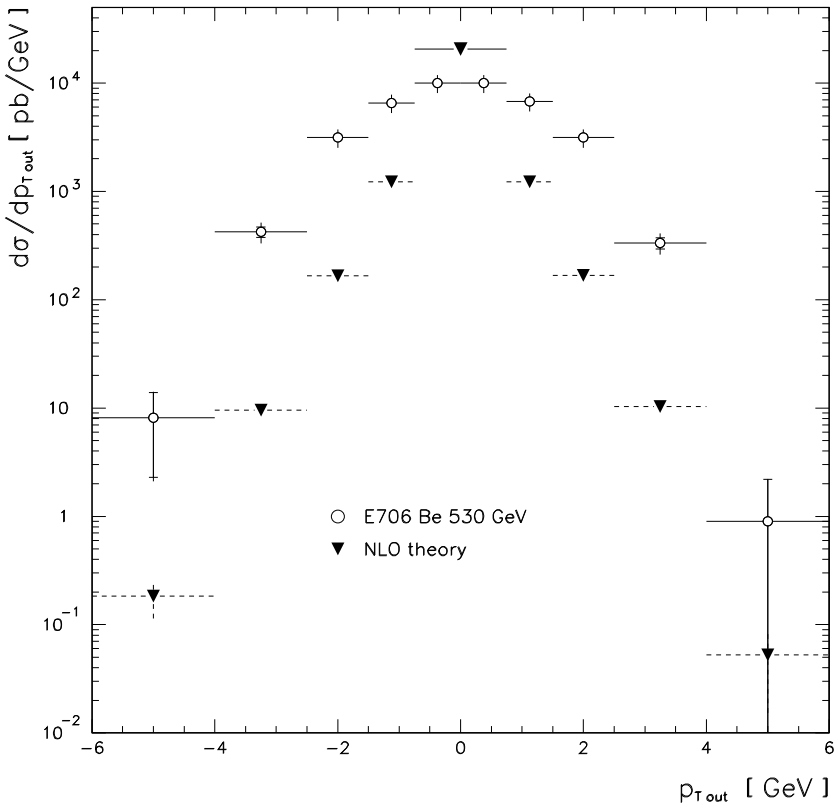

Figure 7: Dipion differential cross section $d\sigma/dp_{T,out}$ vs. the variable $p_{T,out}$ defined in subsect. 3.2, in $p-Be$ collisions with a beam energy of 530 GeV. Data points with statistical and systematic errors in quadrature are from the E706 collaboration [1]. The NLO prediction with scales $M = \mu = M_f = 3/8\,(p_{T1} + p_{T2})$ is shown as triangles.

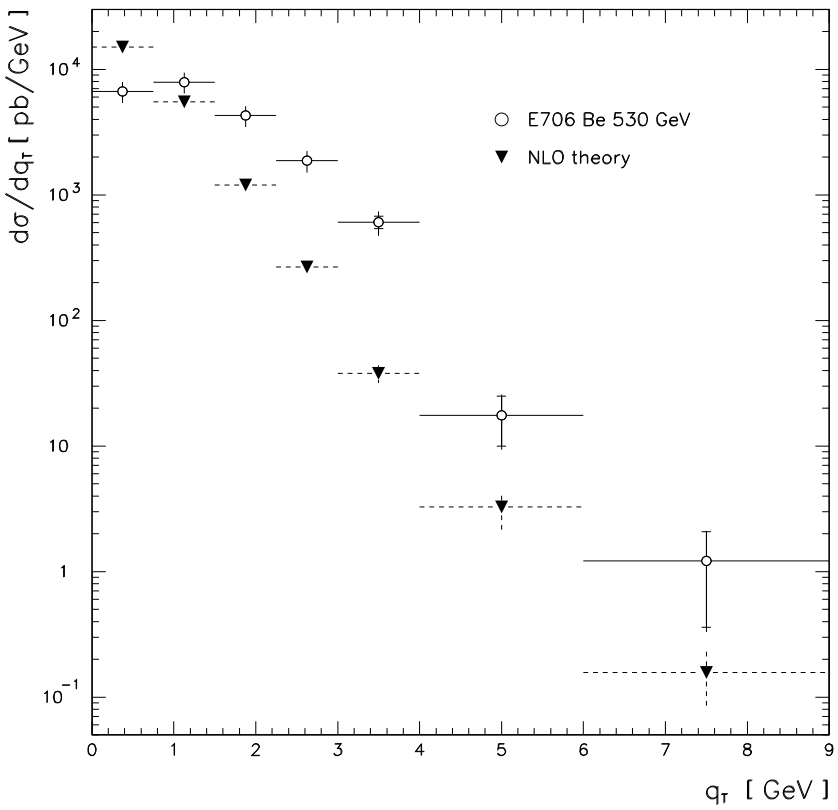

Figure 8: Dipion differential cross section $d\sigma/dq_T$ vs. q_T, the transverse momentum of a pair, in $p - Be$ collisions with a beam energy of 530 GeV. Data points with statistical and systematic errors in quadrature are from the E706 collaboration [1]. The NLO prediction with scales $M = \mu = M_f = 3/8\,(p_{T1} + p_{T2})$ is shown as triangles.

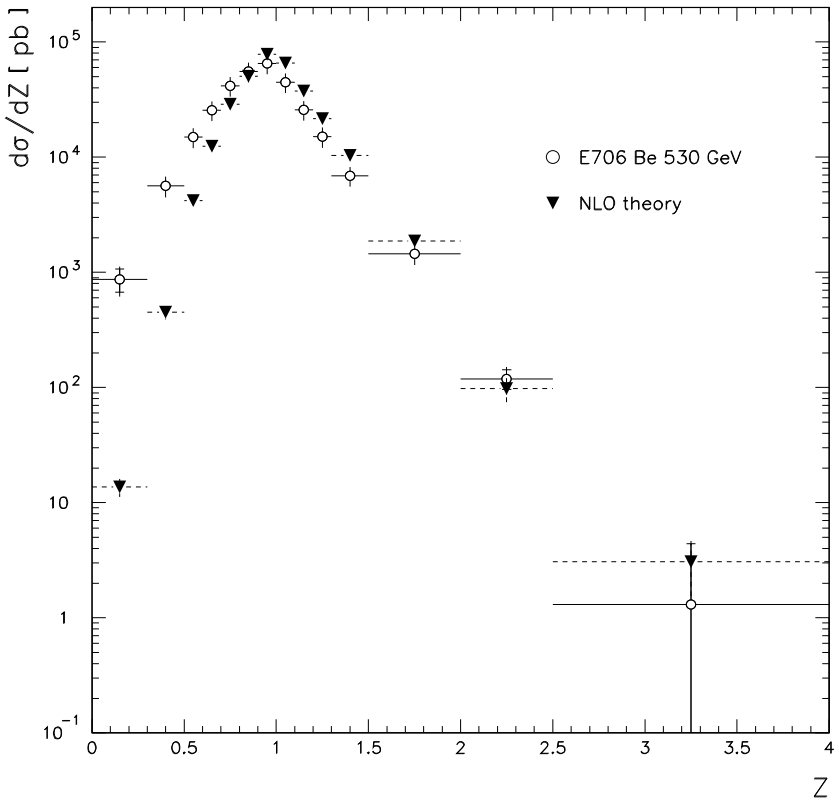

Figure 9: Dipion differential cross section $d\sigma/dZ$ vs. the variable Z defined in subsect. 3.2, in $p - Be$ collisions with a beam energy of 530 GeV. Data points with statistical and systematic errors in quadrature are from the E706 collaboration [1]. The NLO prediction with scales $M = \mu = M_f = 3/8\,(p_{T1} + p_{T2})$ is shown as triangles.

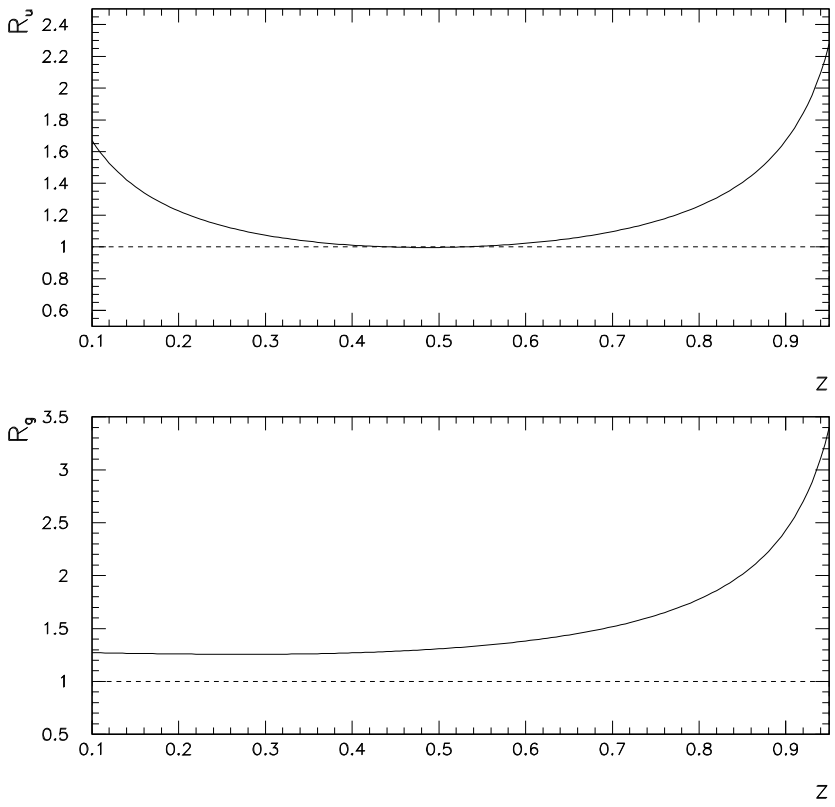

Figure 10: Ratios $R_f(z) = D^{KKP}_{\pi/f}(z, M_f)/D^{BKK}_{\pi/f}(z, M_f)$ of BKK to KKP fragmentations functions, vs. z, for various partons flavours f, at $M_f = 3$ GeV. Top: $f = u$ quark ($f = d$ quark equal to u). Bottom: $f =$ gluon.

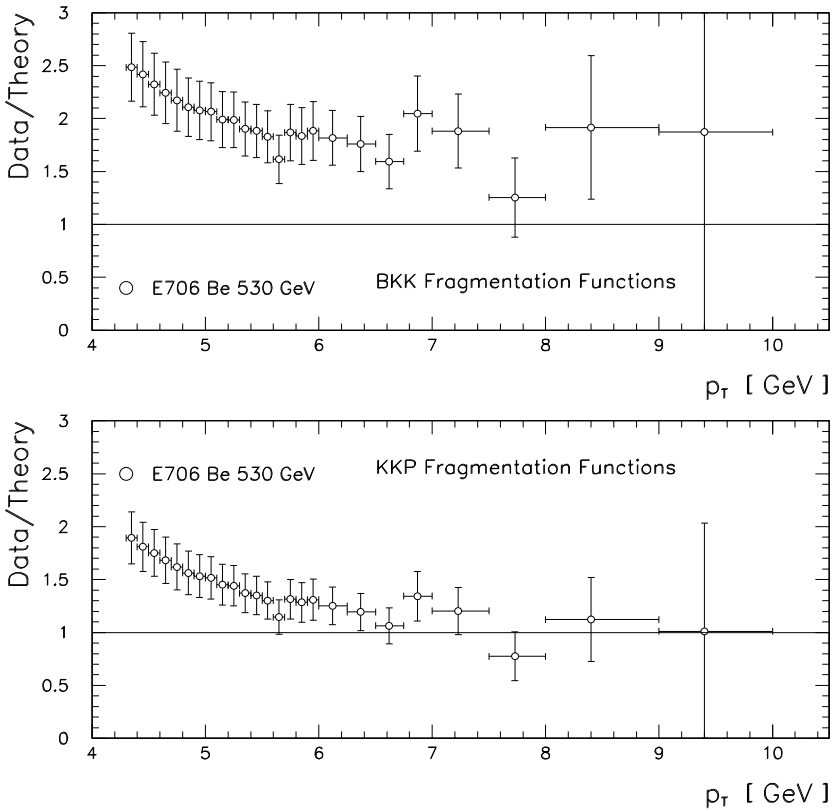

Figure 11: Collisions of 530 GeV protons on Be target. Comparisons of E706 data with NLO predictions for the one pion inclusive p_T spectrum, for BKK and KKP sets of fragmentation functions. The scale choice used is $\mu = M = M_f = p_T/3$. Only data points with $p_T > 4.35$ GeV are kept in order that the fragmentation scale M_f in the NLO predictions is above the starting scale $\sqrt{2}$ GeV of the BKK and KKP sets.

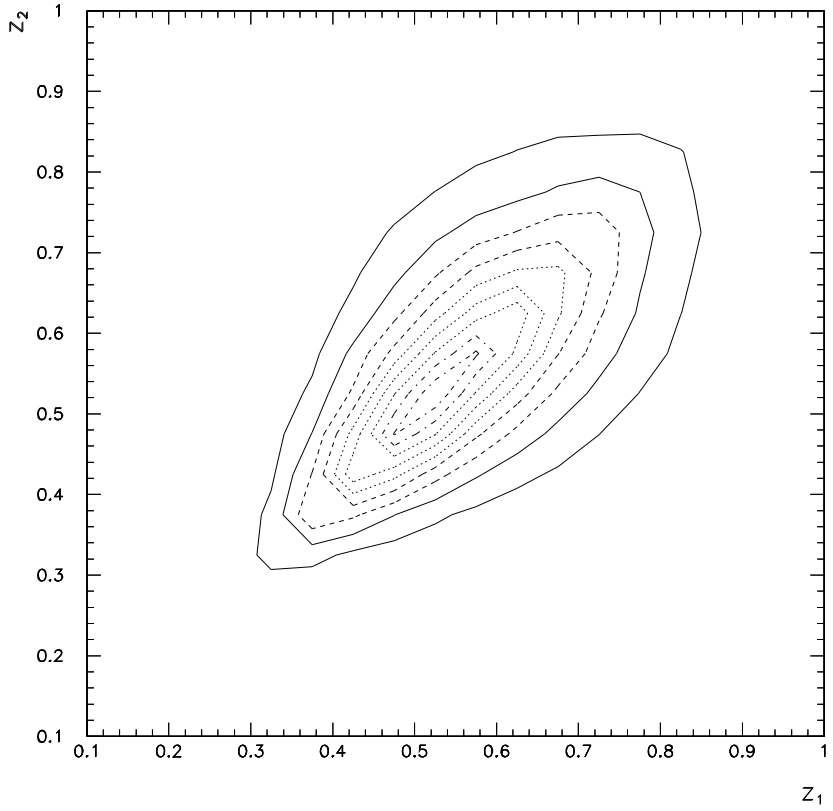

Figure 12: Contour plot of $A = d\sigma/dz_1 dz_2$ in the plane of the longitudinal fragmentation variables (z_1, z_2). The iso-A curves are oriented along the diagonal $z_1 = z_2$. The most inner iso-A curves, centered on the region $z_1 = z_2 \simeq 0.5$ correspond to the largest values of A.

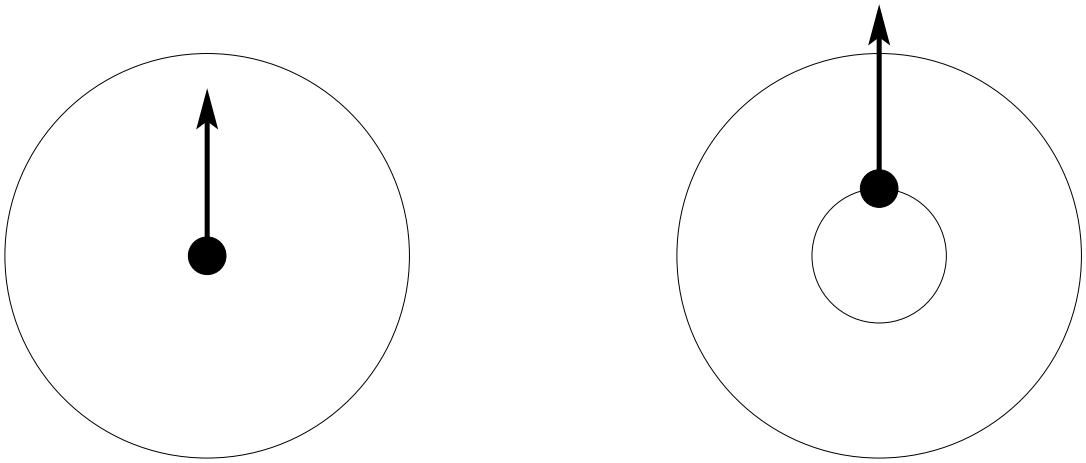

Figure 13: Illustration of trigger bias effect in one particle inclusive production. The large circle has radius $p_{T\,min}$. The thick arrow stands for the transverse momentum of the pion generated by the hard subprocess. Left: pion not hard enough and no k_T kick: event discarded . The radius of the inner circle on the right indicates the magnitude of the k_T kick. Right: the pion would not be produced hard enough, but the partonic subprocess is kicked transversally: event accepted.

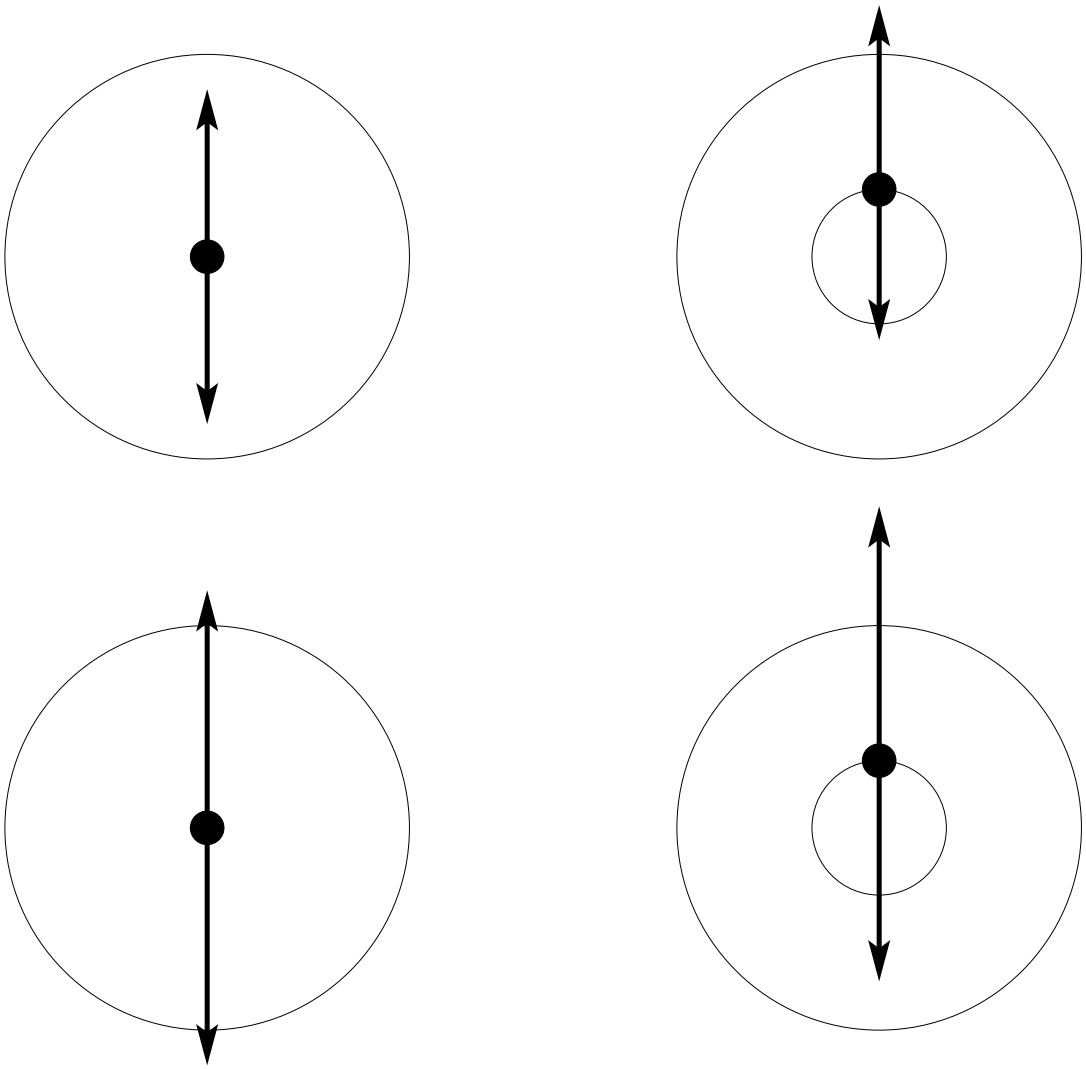

Figure 14: Illustration of the absence of trigger bias effect in inclusive pair production. The large circle has radius $p_{T\,min}$. The thick arrows stand for the transverse momenta of the pions generated by the hard subprocess. The radius of the inner circle on the right indicates the magnitude of the k_T kick. Top: the pions are not produced hard enough by the partonic subprocess. Top left: no k_T kick: event discarded. Top right: one pion is favoured by k_T kick, the other one is penalized: event also discarded. Bottom: the pions would be produced hard enough by the subprocess. Bottom left: no k_T kick, event accepted. Bottom right: one pion is kicked down, even discarded.

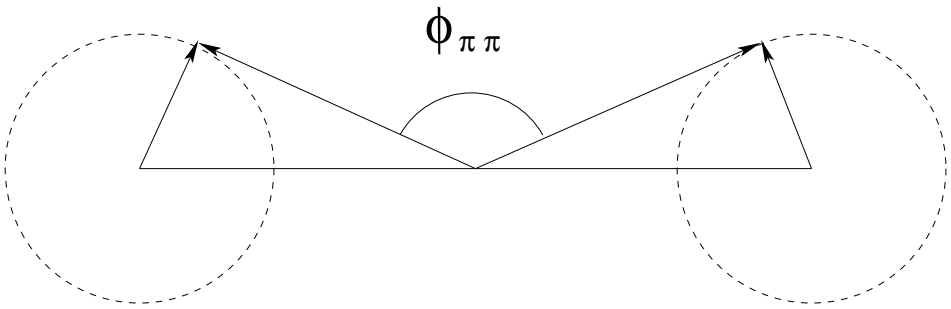

Figure 15: Illustration of the reshuffle of back to back configurations by final state k_T kick. The radii of the circles represent the magnitude of the kick. If the magnitude of the k_T kick is not much smaller than the selection cut $p_{T\,min}$, the $\phi_{\pi\pi}$ of the reshuffled configuration can be very different from π.

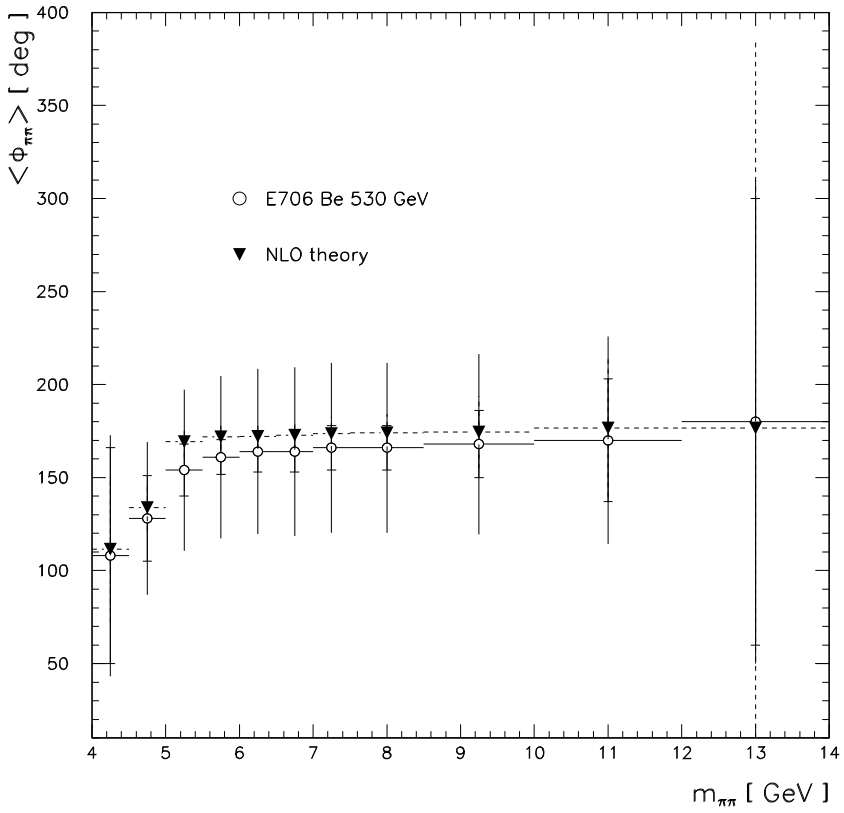

Figure 16: Dipion distribution $< d\phi_{\pi\pi} > /dm_{\pi\pi}$ vs. the invariant mass $m_{\pi\pi}$, in $p - Be$ collisions with a beam energy of 530 GeV. Data points with statistical and systematic errors in quadrature are from the E706 collaboration [1]. The NLO prediction with scales $M = \mu = M_f = 3/8\,(p_{T1} + p_{T2})$ is shown as triangles.

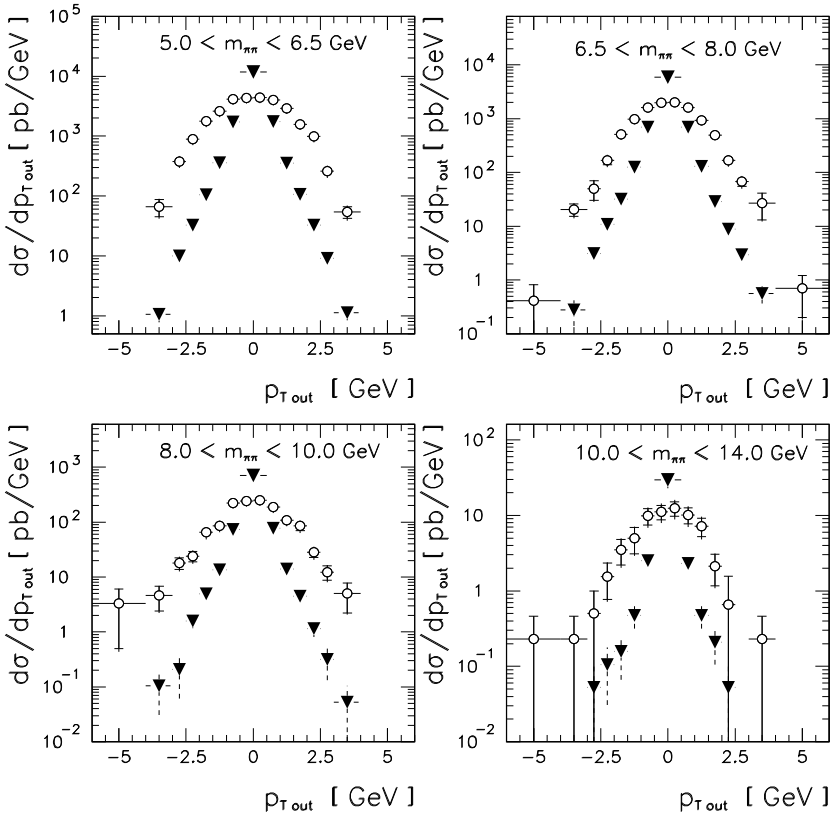

Figure 17: Dipion differential cross section Dipion differential cross section $d\sigma/dp_{T\,out}$ vs. $p_{T\,out}$ in $p-Be$ collisions with a beam energy of 530 GeV. Here $d\sigma/dp_{T\,out}$ stands for $\int dm_{\pi\pi}(d\sigma/dp_{T\,out}dm_{\pi\pi})$ integrated over the following invariant mass slices: $5.0 < m_{\pi\pi} < 6.5$ GeV (top left), $6.5 < m_{\pi\pi} < 6.5$ GeV (top right), $8.0 < m_{\pi\pi} < 10.0$ GeV (bottom left) and $10.0 < m_{\pi\pi} < 14.0$ GeV (bottom right). Data points with statistical and systematic errors in quadrature are from the E706 collaboration [1]. The NLO prediction with scales $M = \mu = M_f = 3/8\,(p_{T1} + p_{T2})$ is shown as triangles.

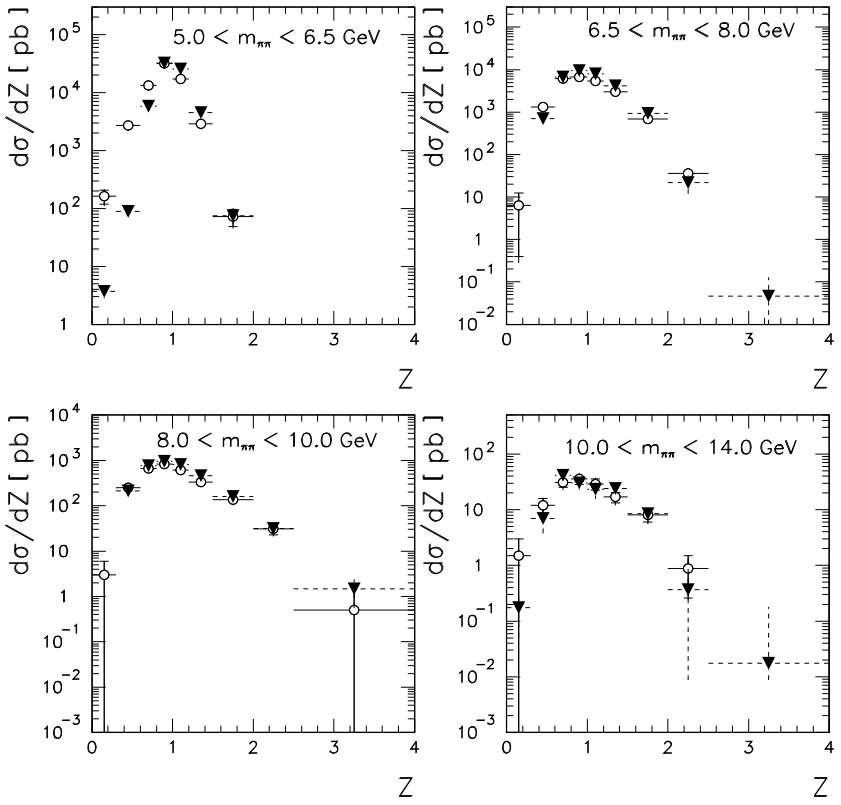

Figure 18: Dipion differential cross section $d\sigma/dZ$ vs. Z in $p-Be$ collisions with a beam energy of 530 GeV. Here $d\sigma/dZ$ stands for $\int dm_{\pi\pi}(d\sigma/dZdm_{\pi\pi})$ integrated over the following invariant mass slices: $5.0 < m_{\pi\pi} < 6.5$ GeV (top left), $6.5 < m_{\pi\pi} < 6.5$ GeV (top right), $8.0 < m_{\pi\pi} < 10.0$ GeV (bottom left) and $10.0 < m_{\pi\pi} < 14.0$ GeV (bottom right). Data points with statistical and systematic errors in quadrature are from the E706 collaboration [1]. The NLO prediction with scales $M = \mu = M_f = 3/8\,(p_{T1} + p_{T2})$ is shown as triangles.